

The MKK3–MPK7 cascade phosphorylates ERF4 and promotes its rapid degradation to release seed dormancy in *Arabidopsis*

Xi Chen^{1,7}, Qiujia Li^{1,7}, Ling Ding¹, Shengnan Zhang², Siyao Shan¹, Xiong Xiong³, Wenhui Jiang¹, Bo Zhao⁴, Liying Zhang¹, Ying Luo⁵, Yiming Lian³, Xiuqin Kong³, Xiali Ding¹, Jun Zhang¹, Chunli Li¹, Wim J.J. Soppe⁶ and Yong Xiang^{1,*}

¹Shenzhen Branch, Guangdong Laboratory for Lingnan Modern Agriculture, Genome Analysis Laboratory of the Ministry of Agriculture, Agricultural Genomics Institute at Shenzhen, Chinese Academy of Agricultural Sciences, Shenzhen 518120, China

²Center for Crop Science, College of Agronomy, Qingdao Agricultural University, Qingdao 266109, China

³School of Petrochemical Engineering, Lanzhou University of Technology, Lanzhou 730050, China

⁴Hou Ji Laboratory in Shanxi Province, Academy of Agronomy, Shanxi Agricultural University, Taiyuan 030031, China

⁵State Key Laboratory of Silkworm Genome Biology, Southwest University, Chongqing 400715, China

⁶Rijk Zwaan, 2678 ZG De Lier, the Netherlands

⁷These authors contributed equally to this article.

*Correspondence: Yong Xiang (xiangyong@caas.cn)

<https://doi.org/10.1016/j.molp.2023.09.006>

ABSTRACT

Seeds establish dormancy to delay germination until the arrival of a favorable growing season. In this study, we identify a fate switch comprised of the MKK3–MPK7 kinase cascade and the ethylene response factor ERF4 that is responsible for the seed state transition from dormancy to germination. We show that dormancy-breaking factors activate the MKK3–MPK7 module, which affects the expression of some α -EXPANSIN (*EXPA*) genes to control seed dormancy. Furthermore, we identify a direct downstream substrate of this module, ERF4, which suppresses the expression of these *EXPAs* by directly binding to the GCC boxes in their exon regions. The activated MKK3–MPK7 module phosphorylates ERF4, leading to its rapid degradation and thereby releasing its inhibitory effect on the expression of these *EXPAs*. Collectively, our work identifies a signaling chain consisting of protein phosphorylation, degradation, and gene transcription, by which the germination promoters within the embryo sense and are activated by germination signals from ambient conditions.

Key words: seed dormancy, dormancy breaking, seed germination, MKK3, MPK7, ERF4, phosphorylation, protein degradation, DNA binding

Chen X., Li Q., Ding L., Zhang S., Shan S., Xiong X., Jiang W., Zhao B., Zhang L., Luo Y., Lian Y., Kong X., Ding X., Zhang J., Li C., Soppe W.J.J., and Xiang Y. (2023). The MKK3–MPK7 cascade phosphorylates ERF4 and promotes its rapid degradation to release seed dormancy in *Arabidopsis*. *Mol. Plant*. **16**, 1–16.

INTRODUCTION

Seed dormancy is a vital adaptive trait of seed plants, and the establishment and breaking of dormancy are critical for plant reproduction and evolution (Koornneef et al., 2002; Née et al., 2017a). Seed dormancy is defined as the failure of a viable seed to germinate under suitable conditions (Bewley, 1997; Baskin and Baskin, 2004). Seed dormancy level is usually assessed by measuring the germination rate of a population of seeds under suitable conditions during after-ripening storage (Soppe and Bentsink, 2020). Both dormancy establishment and release can impact eventual germination rates, and both

processes are influenced by numerous internal and external factors. The phytohormone abscisic acid (ABA), as well as the master dormancy regulators *DELAY OF GERMINATION1* (*DOG1*), *REDUCED DORMANCY5* (*RDO5*), and *REVERSAL OF RDO5 1* (*ODR1*), are representative dormancy-establishment factors; the phytohormone gibberellic acid (GA), as well as cold stratification (CS) and hydrogen peroxide (H_2O_2) treatments, are dormancy-releasing factors (Bentsink et al., 2006; Liu et al.,

Molecular Plant

2010, 2020; Arc et al., 2012; Debska et al., 2013; Xiang et al., 2014, 2016; Née et al., 2017a).

After the release of dormancy, seeds can initiate germination under suitable conditions through an ordered series of morphogenetic processes, starting with uptake of water by the quiescent dry seed (imbibition), followed by embryo expansion, and ending in radicle protrusion (germination) (Bewley, 1997). Embryo expansion is the result of cell elongation rather than cell division in the radicle-adjacent transition zone and lower hypocotyl (Sliwinska et al., 2009; Bassel et al., 2014), which is largely dependent on the expression of diverse cell-wall-modifying gene families, including the α -*EXPANSIN* (*EXPA*) gene subfamily (Cosgrove, 1998; 2000; Holdsworth et al., 2008; Xu et al., 2020). Some *EXPAs* (*EXPA1-3*, *EXPA8-10*, *EXPA13*, *EXPA15*, and *EXPA20*) are specifically and highly expressed in imbibed seeds and can be dramatically induced by dormancy-breaking factors like GA and H₂O₂ during seed imbibition (Schopfer, 2001; Zhong et al., 2015; Xu et al., 2020). Dissecting the expression regulation mechanism of these *EXPAs* during imbibition is therefore critical for understanding the mechanism of dormancy release. However, how seeds transduce external dormancy-breaking signals into downstream *EXPA* expression remains unknown.

Recently, emerging evidence has revealed that one hub of the mitogen-activated protein kinase (MPK) cascades, the MKK3-centered cascade, is crucial for control of seed dormancy. *MKK3* has been identified as the causal gene for a major dormancy QTL in barley and wheat and as a dormancy regulator in rice (Nakamura et al., 2016; Torada et al., 2016; Mao et al., 2019). However, the precise mechanism by which *MKK3* regulates seed dormancy in these crops remains largely unknown. MPK cascades are highly conserved signaling pathways that act downstream of signal receptors/sensors and transduce signals into intracellular events by phosphorylating their substrates, which may play various roles in different biological processes. A canonical MPK cascade consists of three-tiered sequential phosphorylation from MPK kinase kinases (MKKKs) to MPK kinases (MKKs) and finally to MPKs (Tena et al., 2001; Asai et al., 2002; Rodriguez et al., 2010; Xu and Zhang, 2015; Zhang and Zhang, 2022). There are 20, 10, and approximately 80 MPKs, MKKs, and MKKKs, respectively, in *Arabidopsis* (Colcombet and Hirt, 2008). Therefore, the regulatory networks of MPK cascades are extremely complex. The MKK3-centered cascade includes MKKK16–18 and MKKK20 as its upstream MKKKs and the group C MPKs (MPK1–2, MPK7, and MPK14) as its downstream MPKs (Doczi et al., 2007; Lee et al., 2008; Danquah et al., 2015; Matsuoka et al., 2015; Colcombet et al., 2016; Benhamman et al., 2017; Choi et al., 2017; Bai and Matton, 2018). Interestingly, the upstream signal molecules that activate the MKK3-mediated cascade include ABA and H₂O₂ (Doczi et al., 2007; Danquah et al., 2015), which have opposite roles in the control of seed dormancy. The relationship between ABA and MKK3 is subtle: several reports have shown that MKK3 affects ABA signaling but has inconsistent results among different tissues and developmental processes, such as seed germination, root growth, and leaf senescence (Hwa and Yang, 2008; Danquah et al., 2015; Matsuoka et al., 2015; Choi et al., 2017). This

MKK3–MPK7–ERF4 axis regulates seed dormancy

suggests that the role of the MKK3 cascade in ABA signaling is complex and that inconsistencies may be due to different downstream substrates in distinct tissues. However, there are only a few reports on downstream substrates of the MKK3-mediated cascade. Some have suggested that the transcription factor (TF) MYC2, which is phosphorylated by MKK3-activated MPK6, may be a substrate of the MKK3-mediated cascade (Takahashi et al., 2007; Sethi et al., 2014). However, this hypothesis has recently been challenged, as MPK6 has been demonstrated to be an indirect downstream MPK of MKK3 (Doczi et al., 2007; Matsuoka et al., 2015; Sozen et al., 2020). Therefore, it is crucial to identify the substrates of the direct interacting MPKs in the MKK3-mediated cascade to gain a better understanding of its signaling mechanisms and its role in the control of seed dormancy.

Many studies have reported that several ethylene response factors (ERFs) are substrates of MPK cascades (Popescu et al., 2009; Cao et al., 2018; Lv et al., 2021). The ERFs belong to a plant-specific TF family with at least 122 members (Nakano et al., 2006), which have diverse functions in response to various signals in *Arabidopsis*. Among these members, ERF4 may be involved in the control of seed dormancy because it interacts antagonistically with MYB52 to control seed coat mucilage, which is related to seed dormancy (Debeaujon et al., 2000; Zhang et al., 2020; Ding et al., 2021). ERF4 harbors a single AP2/ERF DNA binding domain in its N-terminal region and an ERF-associated amphiphilic repression motif in its C-terminal region, which enable it to bind to the GCC box of its target genes and repress their expression (Fujimoto et al., 2000; Ohta et al., 2001; Yang et al., 2005). The identified targets of ERF4 include three pectin methylesterase inhibitor genes (*PMEI13-15*), *SUBTILISIN-LIKE SERINE PROTEASE 1.7* (*SBT1.7*), and the cell-cycle gene *CYCLIN A2;3* (*CYA2;3*) (Ding et al., 2021, 2022). Few of these genes have been reported to have direct functions in the control of seed dormancy. Whether ERF4 has other substrates involved in dormancy control remains to be determined.

In our previous study, we identified six mutants (*odr1* to *odr6*) that rescue the dormancy-reducing phenotype of *rdo5-2* and reported a role for *ODR1* in the regulation of seed dormancy (Liu et al., 2020). In the present study, we confirm that *odr2* is a knockout allele of *MKK3* in the *rdo5-2* background. Our work reveals that MKK3 and its direct downstream kinase MPK7 act as a functional module that positively controls dormancy release. The MKK3–MPK7 module is activated by dormancy-breaking conditions and subsequently transduces the signal downstream to facilitate *EXPA*-promoted embryo expansion. Further work identified ERF4, which interacts with and is phosphorylated by MPK7, as a direct substrate of this module. ERF4 negatively regulates dormancy release and embryo expansion by directly binding to the GCC box in the exons of *EXPAs* and repressing their expression during seed imbibition. Moreover, MPK7 regulates ERF4 stability through phosphorylation, leading to its rapid degradation via a 26S proteasome-dependent pathway. Our results reveal how the MKK3–MPK7–ERF4 signaling chain transduces external dormancy-breaking signals into the cell nucleus of the embryo. These findings reveal the mechanism by which a dormant seed is awakened by environmental signals. Our work can provide theoretical guidance for the creation of crops with suitable

MKK3–MPK7–ERF4 axis regulates seed dormancy

Molecular Plant

dormancy characteristics by gene editing and other bioengineering technologies in the future.

RESULTS

The MKK3–MPK7 module negatively regulates seed dormancy

In our previous study, we identified six mutants (*odr1* to *odr6*) in the *rdo5-2* background with enhanced dormancy levels and reported the role of *ODR1* in the regulation of seed dormancy (Liu et al., 2020). Here, we continued this study and focused on *ODR2*. The *odr2* mutant, which rescues the dormancy-reducing phenotype of *rdo5-2*, has a 1-bp deletion in the second exon of the *MKK3* (AT5G40440) locus that causes a premature stop codon (supplemental Figure 1A and 1B). To confirm that *MKK3* is indeed *ODR2*, we obtained the *mkk3-1* mutant, a loss-of-function mutant of *MKK3* in the Col-0 background (Doczi et al., 2007; Takahashi et al., 2007), and produced the *mkk3-1 rdo5-2* double mutant by crossing. Germination assays showed that loss of *MKK3* function significantly enhances seed dormancy and rescues the *rdo5-2* phenotype (Figure 1A), confirming that *MKK3* is *ODR2* and negatively regulates seed dormancy. After storage for 26 weeks, the *mkk3-1* seeds could germinate completely (Figure 1A), confirming that the dormancy-enhancing phenotype was not due to a loss of seed vitality.

The Group C MPKs (MPK1, MPK2, MPK7, and MPK14) have been identified as direct downstream MPKs of *MKK3* (Doczi et al., 2007), prompting us to investigate their roles in the control of seed dormancy. We obtained homozygous T-DNA insertion mutants for each *MPK*, except for *mpk7*, for which we generated three knockout mutants (named *mpk7_ko1* to *ko3*) using the CRISPR–Cas9 genome-editing technique (supplemental Figure 1C). Germination assays revealed that all three *mpk7* mutants exhibited significantly enhanced seed dormancy levels, whereas the other *MPK* mutants were similar to wild-type Col-0 (Figure 1B). To investigate the possibility of functional redundancy, we constructed various combinations of double and triple *mpks* mutants and found that knockout of *MPK7* is necessary to enhance seed dormancy level (Figure 1C). Furthermore, RNA-seq and microarray data analysis showed that *MPK7* had the highest expression level among the four *MPKs* in both developing and germinating seeds (Figure 1D; supplemental Figure 1D). These results revealed the critical role of *MPK7* among the four *MPKs* in regulation of seed dormancy. The MKK3–MPK7 cascade therefore constitutes a critical module in seed dormancy regulation of *Arabidopsis*. To confirm this hypothesis, we generated homozygous mutants with single-copy T-DNA insertions for *MKK3*OE (35Spro-MKK3-GFP) and *MKK3*^{EE}OE (35Spro-MKK3^{EE}-GFP; EE, S235E and T241E, a constitutively active mutant form of *MKK3*; Doczi et al., 2007) in the *Ler* background and *MPK7*OE (35Spro-MPK7-GFP) in the Col-0 background. We selected three independent lines of each transgenic material for a seed dormancy assay. The results showed that overexpression of *MKK3* and *MPK7* significantly reduced seed dormancy levels (Figure 1E and 1F). Interestingly, overexpression of *MKK3*^{EE} dramatically increased seed germination ability (Figure 1G), implying that the kinase activity of *MKK3* was important for its function in seed dormancy regulation.

The MKK3–MPK7 module acts downstream of dormancy-breaking factors and independently of dormancy-establishment factors

The phytohormone GA plays a crucial role in dormancy release. To determine whether the dormancy-enhancing phenotypes of *mkk3-1* and *mpk7_ko3* could be restored by exogenous GA, we performed germination assays with GA treatment. The results showed that the germination abilities of the mutants could not be effectively recovered by GA application and that they were less sensitive to GA-induced dormancy breaking than wild-type Col-0 (Figure 2A). Moreover, expression of GA homeostasis-related genes in dry and imbibed mutant seeds was in general not significantly different from that of Col-0 seeds (supplemental Figure 2A). These results suggest that the MKK3–MPK7 module is required for GA-triggered dormancy breaking and does not regulate seed dormancy through the GA metabolism pathway. Another effective method for breaking seed dormancy is CS, which activates GA biosynthesis (Yamauchi et al., 2004). Similar to GA treatment, CS treatment did not effectively recover the germination abilities of *mkk3-1* and *mpk7_ko3*, and these mutants were less sensitive to CS than wild-type Col-0 (Figure 2B). This result indicates that the MKK3–MPK7 module is also required for CS-induced dormancy breaking. Overall, these results suggest the possibility of a common signal molecule that activates the MKK3–MPK7 cascade upon GA and CS treatments.

H₂O₂, a pivotal regulator of dormancy release, can be produced rapidly during seed imbibition and further accumulates in response to GA and CS treatments (Oracz et al., 2009; Leymarie et al., 2012; Bailly, 2019; Jurdak et al., 2022). Moreover, H₂O₂ treatment can activate *MPK7* by *MKK3* in *Arabidopsis* protoplasts (Doczi et al., 2007). We therefore hypothesized that H₂O₂ might be the signal molecule that activates the MKK3–MPK7 module during seed imbibition. To test this hypothesis, we investigated whether the MKK3–MPK7 module was required for H₂O₂-triggered dormancy breaking. As expected, both mutants showed less sensitivity to H₂O₂ treatment than wild-type Col-0 (Figure 2C). We also examined the responses of transcript and protein abundance in the MKK3–MPK7 module to these dormancy-releasing conditions. qRT–PCR and immunoblot results indicated a slight effect on RNA and protein abundance (supplemental Figure 2B; Figure 2D). We then examined the kinase activity of *MPK7* in response to these conditions by detecting activated *MPK7* using an anti-pTEpY antibody (Jalmi and Sinha, 2016). The results showed that all conditions significantly increased the kinase activity of *MPK7* by two- to three-fold (Figure 2E). These data suggest that the MKK3–MPK7 module works downstream of H₂O₂, as well as downstream of the GA and CS treatments that produce H₂O₂. The data also highlighted the importance of *MPK7* kinase activity in this module.

We also assessed the relationship between the MKK3–MPK7 module and some important dormancy-establishment factors, such as ABA, *DOG1*, and *RDO5*. ABA is essential for seed dormancy establishment and exhibits bidirectional interactions with *MKK3*-mediated cascades (Hwa and Yang, 2008; Danquah et al., 2015; Matsuoka et al., 2015; Née et al., 2017a; Choi et al., 2017). To clarify the interaction between the MKK3–MPK7 module and ABA signaling in seed dormancy regulation, we compared ABA sensitivity and dormancy levels of *mkk3-1* and *mpk7_ko3* mutants with those of a knockout mutant

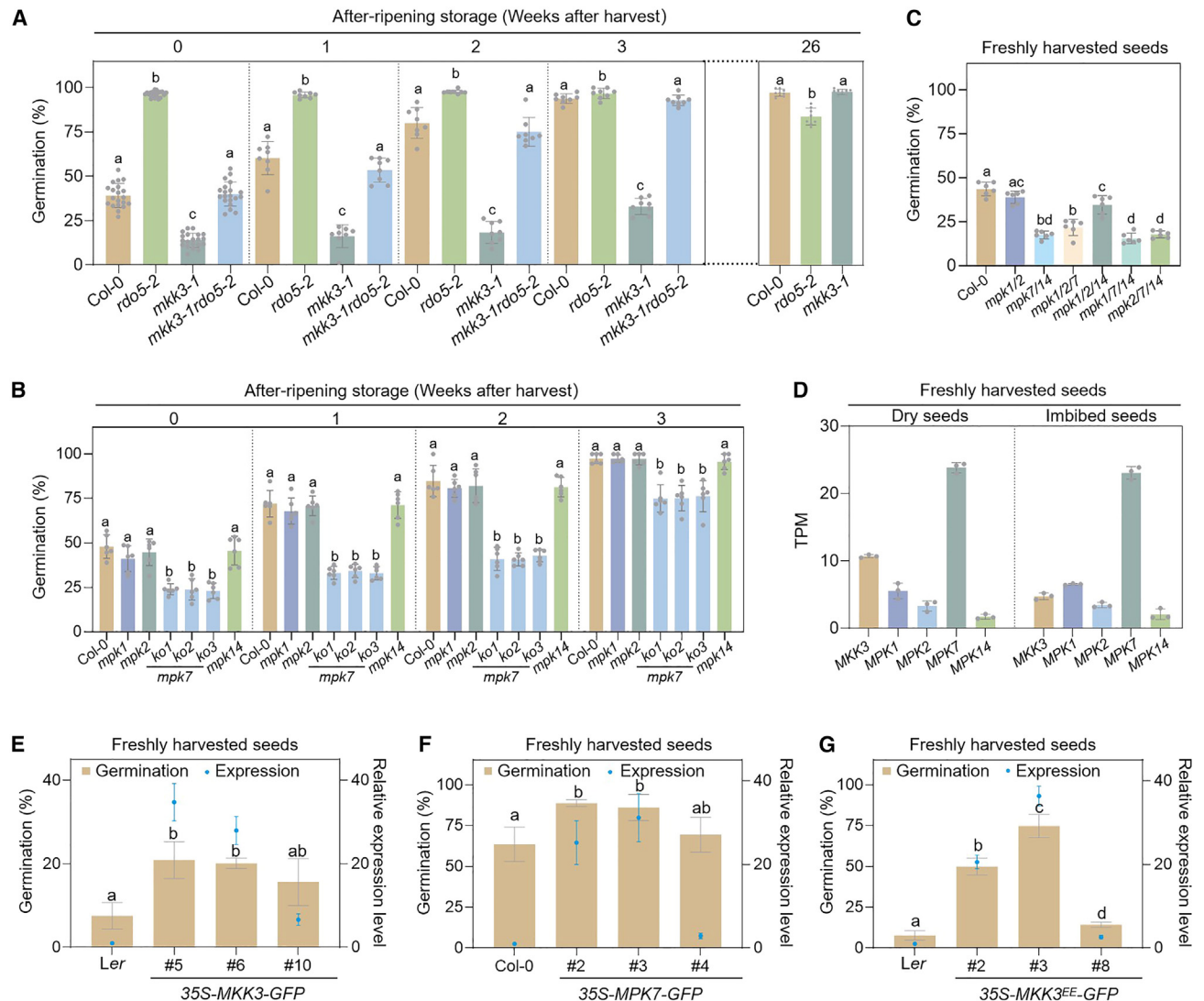


Figure 1. The MKK3-MPK7 module negatively regulates seed dormancy.

(A–C) Germination assays with seeds from different genetic backgrounds. The germination rates were calculated after 7 days of incubation under 16-h light/8-h dark (23°C/20°C) conditions. Data are represented as means ± SD of at least six independent replicates. Each dot represents the value from one replicate. Lowercase letters indicate statistically distinct groups ($p < 0.05$, Student's t -test).

(D) Expression levels of *MKK3*, *MPK1*, *MPK2*, *MPK7*, and *MPK14* in freshly harvested dry and 6-h imbibed seeds detected by RNA-seq assays. Expression levels are represented as TPM (transcripts per million). Data are represented as means ± SD of three independent replicates. Each dot represents the value from one replicate.

(E–G) Germination assays with seeds from overexpression lines of *MKK3*^{WT} (E), *MPK7*^{WT} (F), and *MKK3*^{EE} (G). The germination rates were calculated after 7 days of incubation under 16-h light/8-h dark (23°C/20°C) conditions. Data are represented as means ± SD of three independent replicates. Lowercase letters indicate statistically distinct groups ($p < 0.05$, Student's t -test). The right y axis indicates the expression level of *MKK3* (E or G) and *MPK7* (F) in overexpression lines. See also supplemental Figure 1.

(*ahg1-5*) of *AHG1*, a critical negative component of the ABA signaling pathway and a seed dormancy regulator (Nishimura et al., 2007; Née et al., 2017b). Our findings revealed that the ABA sensitivity of *mkk3-1* and *mpk7_ko3* was higher than that of Col-0 but significantly weaker than that of *ahg1-5* (Figure 2F). However, the seed dormancy levels of *mkk3-1* and *mpk7_ko3* were similar to or even higher than that of *ahg1-5* (Figure 2G). Furthermore, expression levels of core ABA signaling components were very similar between the two mutants and Col-0 (supplemental Figure 2A). These findings collectively suggest that, in the context of suitable germination conditions

that do not involve exogenous ABA application, the effect of the MKK3-MPK7 module on ABA signal transduction may not be as significant as that of core ABA signaling components such as *AHG1*. Therefore, the slightly altered ABA signaling observed in *mkk3-1* and *mpk7_ko3* may not be the primary contributor to their pronounced enhancement of seed dormancy.

DOG1 and *RDO5* are master regulators of seed dormancy establishment, and their expression levels during seed maturation are both correlated with seed dormancy levels (Nakabayashi et al., 2012; Xiang et al., 2014). Many genes control seed dormancy

MKK3-MPK7-ERF4 axis regulates seed dormancy

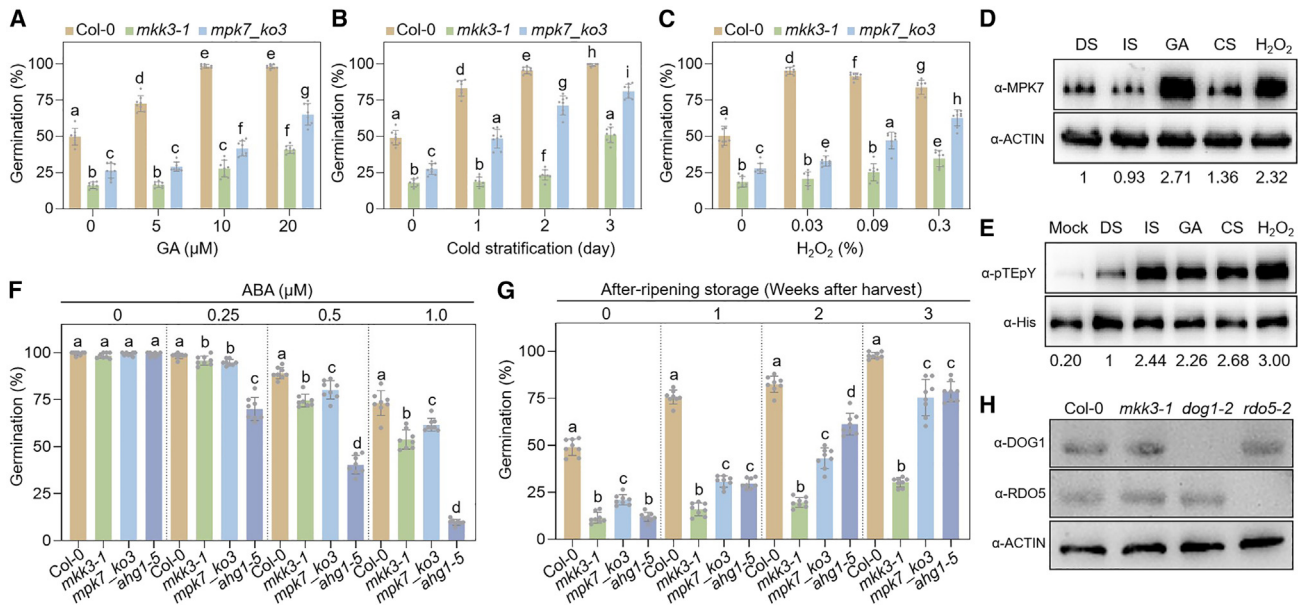


Figure 2. The MKK3-MPK7 module acts downstream of dormancy-breaking factors and independently of dormancy-establishment factors.

(A–C) Germination assays showing the response of *mkk3-1* and *mpk7_ko3* to dormancy-breaking factors during seed germination. Freshly harvested seeds were imbibed in water containing the indicated concentrations of GA (A) or H₂O₂ (C) or were pre-imbibed at 4°C for the indicated number of days before transfer to normal conditions (B). The germination rates were calculated after 7 days of incubation under 16-h light/8-h dark (23°C/20°C) conditions. Data are represented as means ± SD of eight independent replicates. Each dot represents the value from one replicate. Lowercase letters indicate statistically distinct groups (*p* < 0.05, Student’s *t*-test).

(D) MPK7 protein abundance in response to dormancy-breaking factors as detected in immunoblot assays using MPK7 antibody. Protein samples were extracted from Col-0 seeds after 24 h of treatments with the indicated conditions. ACTIN was used as an internal reference. Numbers below the image show the gray value ratio of the MPK7 band compared with the ACTIN band as calculated with ImageJ.

(E) Response of MPK7 kinase activity to dormancy-breaking factors. Recombinant His-MPK7 protein was incubated with seed protein solutions for kinase reactions; the extraction buffer was used as a control. Abundance of His-MPK7 and phosphorylated His-MPK7 was detected with anti-His and anti-pTEpY antibodies, respectively. Numbers are the gray value ratios of the phosphorylated His-MPK7 band compared with the His-MPK7 band as calculated with ImageJ. The ratio in DS was normalized as “1.”

(F and G) ABA sensitivity during germination (F) and seed dormancy levels (G) of *mkk3-1*, *mpk7_ko3*, and *ahg1-5*. In (F), after-ripened seeds were sown onto 1/2 MS plates containing the indicated concentration of ABA. In (G), after-ripening seeds were imbibed with water. The germination rates were calculated after 7 days of incubation under 16-h light/8-h dark (23°C/20°C) conditions. Data are represented as means ± SD of eight independent replicates. Each dot represents the value from one replicate. Lowercase letters indicate statistically distinct groups (*p* < 0.05, Student’s *t*-test).

(H) The abundance of RDO5 and DOG1 in freshly harvested *mkk3-1* seeds detected by immunoblot assays. The abundance of DOG1, RDO5, and ACTIN was detected with anti-DOG1, anti-RDO5, and anti-plant actin antibodies, respectively, and ACTIN was used as an internal reference. In (D), (E), and (H), a representative image of three replicates with similar results is shown. DS, dry seeds; IS, seeds imbibed in water; GA, seeds imbibed in 100 μM GA; CS, seeds imbibed in water at 4°C; H₂O₂, seeds imbibed in 0.3% H₂O₂. See also supplemental Figure 2.

by regulating *DOG1* expression levels (Mortensen and Grasser, 2014; Bryant et al., 2019; Li et al., 2019; Chen et al., 2020). However, our results showed that expression of *DOG1* and *RDO5*, including their RNA and protein levels, were not obviously changed in the *mkk3-1* mutant (supplemental Figure 2C; Figure 2H). Furthermore, MKK3 did not interact with either *DOG1* or *RDO5* in a yeast two-hybrid assay (supplemental Figure 2D). Therefore, the MKK3-centered cascade involved in dormancy regulation is probably independent of *DOG1*/*RDO5*. Collectively, these results imply that the MKK3-MPK7 module mainly plays its role during dormancy release rather than dormancy establishment.

The MKK3-MPK7 module affects and relies on downstream EXPAs in releasing dormancy

To identify potential effectors downstream of the MKK3-MPK7 module, we carefully analyzed our RNA-seq data and found

that the induction of nine *EXPAs* (*EXPA1-3*, *EXPA8-10*, *EXPA13*, *EXPA15*, and *EXPA20*) during seed imbibition was suppressed in *mkk3-1* and *mpk7_ko3* (Figure 3A; supplemental Dataset 1). These *EXPAs* are highly expressed during seed imbibition, dramatically induced by GA and H₂O₂ treatments, and essential for cell expansion (Cosgrove, 2000; Muller et al., 2009; Zhong et al., 2015; Xu et al., 2020). We confirmed this finding using qRT-PCR and found that induction of most of these *EXPAs* by dormancy-breaking treatments was also suppressed in both mutants (Figure 3B). Therefore, we speculated that these *EXPAs* act as downstream effectors of the MKK3-MPK7 module. To test this hypothesis, we measured cell length in the radicle-adjacent transition zone and lower hypocotyl during seed imbibition and calculated cell elongation rates (Sliwinski et al., 2009; Bassel et al., 2014). We found that loss of *MKK3* and *MPK7* function hindered *EXPA*-promoted cell elongation in both zones after 6 and 12 h of imbibition (Figure 3C). Overexpression of some of these *EXPAs* (*EXPA1*, *EXPA8-9*,

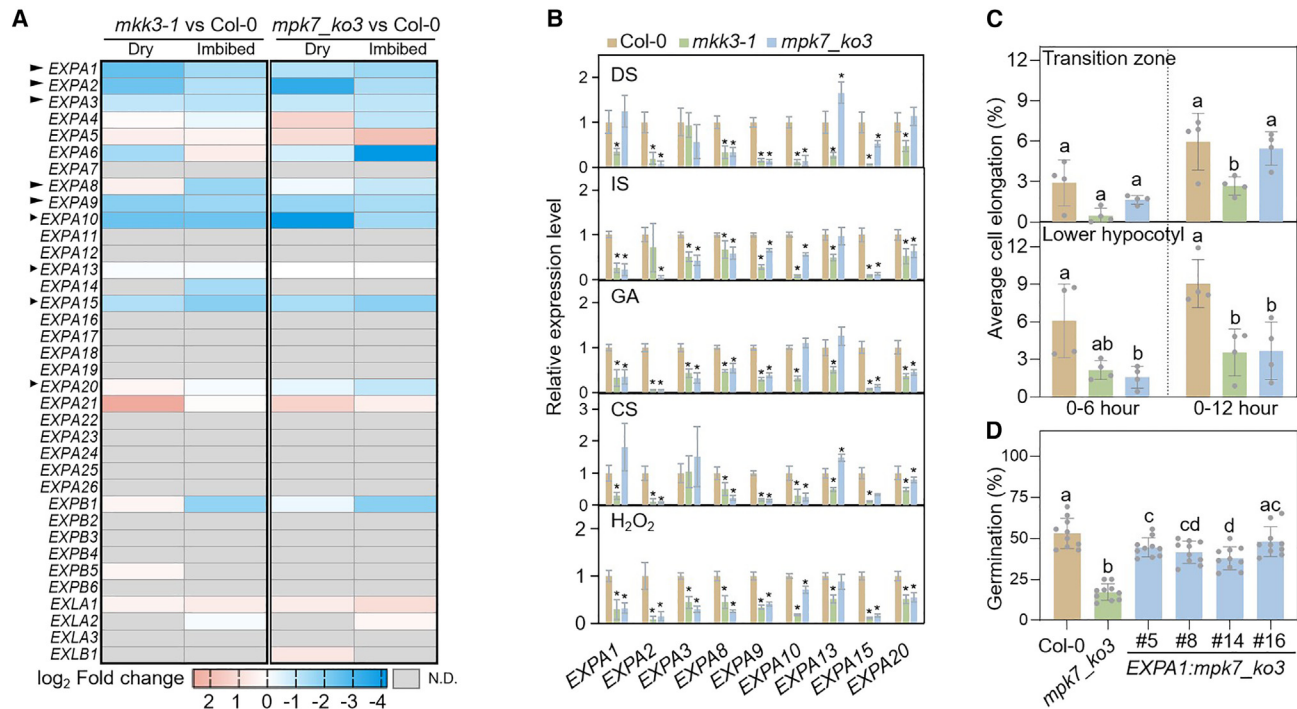


Figure 3. The MKK3-MPK7 module affects and relies on downstream EXPAs in breaking dormancy.

(A) Heatmap showing changes in expression of EXP family members in dry and 6-h imbibed seeds of *mkk3-1* and *mpk7_ko3* compared with Col-0 seeds. The heatmap is based on \log_2 (fold change) values from RNA-seq.

(B) Expression of EXPAs in *mkk3-1* and *mpk7_ko3* seeds after 6 h of treatment with different dormancy-breaking factors detected by qRT-PCR. *ACTIN8* was used as an internal reference. Data are represented as means \pm SD of three independent replicates. * Indicates statistically distinct groups ($p < 0.05$, Student's *t*-test) relative to Col-0. DS, dry seeds; IS, seeds imbibed in water; GA, seeds imbibed in 100 μ M GA; CS, seeds imbibed in water at 4°C; H₂O₂, seeds imbibed in 0.3% H₂O₂.

(C) Cell elongation rate of the radicle-adjacent transition zone and lower hypocotyl of *mkk3-1* and *mpk7_ko3*. The average cell elongation rate was calculated by dividing the relative values of cell elongation after 6- or 12-h imbibition by the cell length at 0 h. Four plants of each genotype were used as biological replicates. For each plant, three to four embryos were measured to capture the variability within the genetic material. Within each embryo, the lengths of five individual cells were measured to obtain representative data. Lowercase letters indicate statistically distinct groups ($p < 0.05$, Student's *t*-test).

(D) Germination assays with seeds overexpressing *EXPA1* in the *mpk7_ko3* background. The germination rates were calculated after 7 days of incubation under 16-h light/8-h dark (23°C/20°C) conditions. Data are represented as means \pm SD of 10 independent replicates. Each dot represents the value from one replicate. Lowercase letters indicate statistically distinct groups ($p < 0.05$, Student's *t*-test). See also [supplemental Figure 3](#).

EXPA13, and *EXPA15*) resulted in a dormancy-attenuating phenotype ([supplemental Figure 3A](#)). We then overexpressed *EXPA1* and *EXPA13* in the *mpk7_ko3* mutant and rescued its dormancy-enhancing phenotype to varying degrees ([Figure 3D](#); [supplemental Figure 3B](#)). These findings demonstrate that the MKK3-MPK7 module facilitates embryo expansion during seed imbibition by promoting expression of these EXPAs.

ERF4 is a substrate of MPK7

We speculated that the kinase MPK7 controls gene expression through its substrates, which may be TFs. To identify potential substrates, we performed a yeast two-hybrid screen with an *Arabidopsis* TF library using MPK7 as bait. Several positive TFs were identified, including the ethylene-responsive element binding factor ERF4, which is highly expressed in seeds and controls seed coat mucilage adhesiveness, a trait related to seed dormancy ([Debeaujon et al., 2000](#); [Zhang et al., 2020](#); [Ding et al., 2021](#)). We confirmed the interaction between MPK7 and

ERF4 *in vitro* using direct yeast two-hybrid and GFP pull-down assays ([Figure 4A](#) and [4B](#)). To further confirm the interaction *in vivo*, we performed co-immunoprecipitation (Co-IP) assays using seeds from transgenic plants expressing a YFP-ERF4 fusion protein driven by the 12S promoter ([Wang et al., 2016](#)). The results demonstrated that YFP-ERF4 interacts with MPK7 in seeds ([Figure 4C](#)).

To determine whether ERF4 is also a substrate of MPK7, we performed a non-radioactive *in vitro* labeling assay ([Leissing et al., 2016](#)). The results of this assay showed that recombinant His-MPK7 could phosphorylate His-ERF4 ([Figure 4D](#)). A sequence analysis identified three potential serine (S) phosphorylation sites in ERF4 (S98, S109, and S173) ([Sharrocks et al., 2000](#)). We mutated all three serine residues to alanine (A) in the recombinant His-ERF4^{AAA} protein to mimic the non-phosphorylated state of ERF4 and found that the mimic protein was not phosphorylated by His-MPK7 ([Figure 4D](#)). This strongly suggests the conservation and significance of the phosphorylation sites. Together, these results indicate that

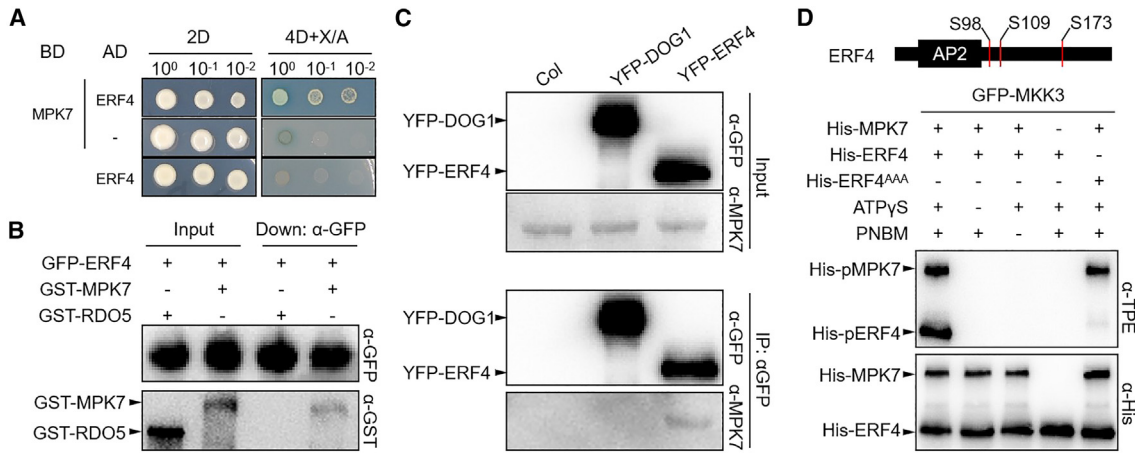


Figure 4. The transcription factor ERF4 is a substrate of MPK7.

(A) Yeast two-hybrid assays confirm that MPK7 interacts with ERF4 in yeast. 2D, double-dropout medium lacking Leu and Trp. 4D, quadruple-dropout medium lacking Ade, His, Leu, and Trp. X, 4 mg/ml X-α-Gal. A, 200 ng/ml AbA.

(B) GFP pull-down assays detect the interaction between GST-MPK7 and GFP-ERF4 *in vitro*. GST-MPK7 and GST-RDO5 were incubated with and pulled down by the GFP-ERF4-bound beads. GST-RDO5 was used as a negative control.

(C) Co-IP assays detect the interaction between MPK7 and YFP-ERF4 *in vivo*. Before protein extraction, seeds were incubated in protein enrichment buffer containing MG132 for 12 h. A transgenic line expressing the YFP-DOG1 fusion protein driven by the DOG1 native promoter was used as a negative control.

(D) Non-radioactive *in vitro* labeling assays show that ERF4 is phosphorylated by MPK7. A diagram shows the exact location of the three potential phosphorylation sites mutated from Ser (S) to Ala (A) in ERF4^{AAA}. The recombinant His-MPK7 protein was activated by GFP-MKK3 and subsequently incubated with His-ERF4 or its non-phosphorylated mimic protein His-ERF4^{AAA} in kinase reactions containing ATPγS or p-nitrobenzyl mesylate (PNBM). ATPγS and PNBM were used to thiophosphorylate ERF4 and alkylate the potential thiophosphoryl group on ERF4, respectively. The thiophosphorylated proteins were detected by an anti-thiophosphate ester (TPE) antibody. In **(A)–(D)**, a representative image of three replicates with similar results is shown.

ERF4 is a direct substrate of MPK7 and suggest that MPK7 may regulate seed dormancy by phosphorylating ERF4, which may in turn regulate the expression of downstream genes.

ERF4 is a dormancy regulator that suppresses embryo expansion

To investigate the role of *ERF4* in regulating seed dormancy, we performed germination assays using two *ERF4* knockout mutants (*erf4-1* and *erf4-2*) (Ding et al., 2021), as well as transgenic lines constitutively expressing YFP-ERF4 in seeds. The two knockout mutants had reduced dormancy levels, whereas the overexpression lines showed enhanced seed dormancy (Figure 5A and 5B), indicating that ERF4 positively regulates dormancy. To confirm that *ERF4* plays a role during seed imbibition, similar to the MKK3-MPK7 module, we used a transgenic line that can induce *ERF4* expression upon β-estradiol treatment (Coego et al., 2014). We observed that increased expression of *ERF4* during imbibition led to decreased germination rates (Figure 5C), confirming the repressive role of *ERF4* in germination.

A previous study has shown that ERF4 regulates the adhesiveness of seed coat mucilage during imbibition (Ding et al., 2021), suggesting that the seed coat might contribute to the regulation of dormancy by ERF4. To assess whether the embryo also makes a contribution, we performed a crossing test. Interestingly, germination of F1 seeds from the cross ♀*erf4-1* × ♂Col-0 (homozygous *erf4-1* seed coat and heterozygous embryo) was indistinguishable from that of ♀Col-0 × ♂Col-0 (supplemental Figure 4), indicating that the embryo plays a major role in the regulation of dormancy by ERF4.

We then measured cell length in the radicle-adjacent transition zone and lower hypocotyl and calculated cell elongation rate to investigate whether *ERF4* affected cell expansion during seed imbibition, similar to the MKK3-MPK7 module. The elongation rate of the *erf4-1* mutant was three- to four-fold higher than that of Col-0 and nearly eight-fold higher than that of the *mkk3-1* and *mpk7_ko3* mutants after 12 h imbibition (Figure 5D). This result indicates that ERF4 and the MKK3-MPK7 module control cell expansion in opposite directions. We also observed that the initial cell length of the *erf4-1* embryo was shorter than that of Col-0 (Figure 5D), consistent with a previous report that ERF4 increases cell size by suppressing the expression of cell-cycle genes such as *CYCA2;3* (Ding et al., 2022). However, our RNA-seq data showed that most of these cell-cycle genes were expressed at extremely low levels in seeds and were not affected by ERF4 (supplemental Figure 5; supplemental Dataset 2). Thus, ERF4 may control cell elongation in the seed embryo through the EXPAs rather than the cell-cycle genes. Overall, our results indicate that ERF4 plays a critical role in regulating seed dormancy and embryo cell elongation, potentially through an EXPA-mediated pathway.

ERF4 directly binds to EXPAs and suppresses their expression

To test this hypothesis, we examined the expression of EXPAs in dry and imbibed seeds of *erf4-1* and Col-0. Expression of *EXPA1-3*, *EXPA8-10*, and *EXPA15* was significantly increased in *erf4-1* (Figure 6A; supplemental Dataset 2), suggesting that ERF4 may inhibit their expression. ERF4 typically binds to the GCC box of its targets and suppresses their expression (Fujimoto et al., 2000; Ohta et al., 2001; Yang

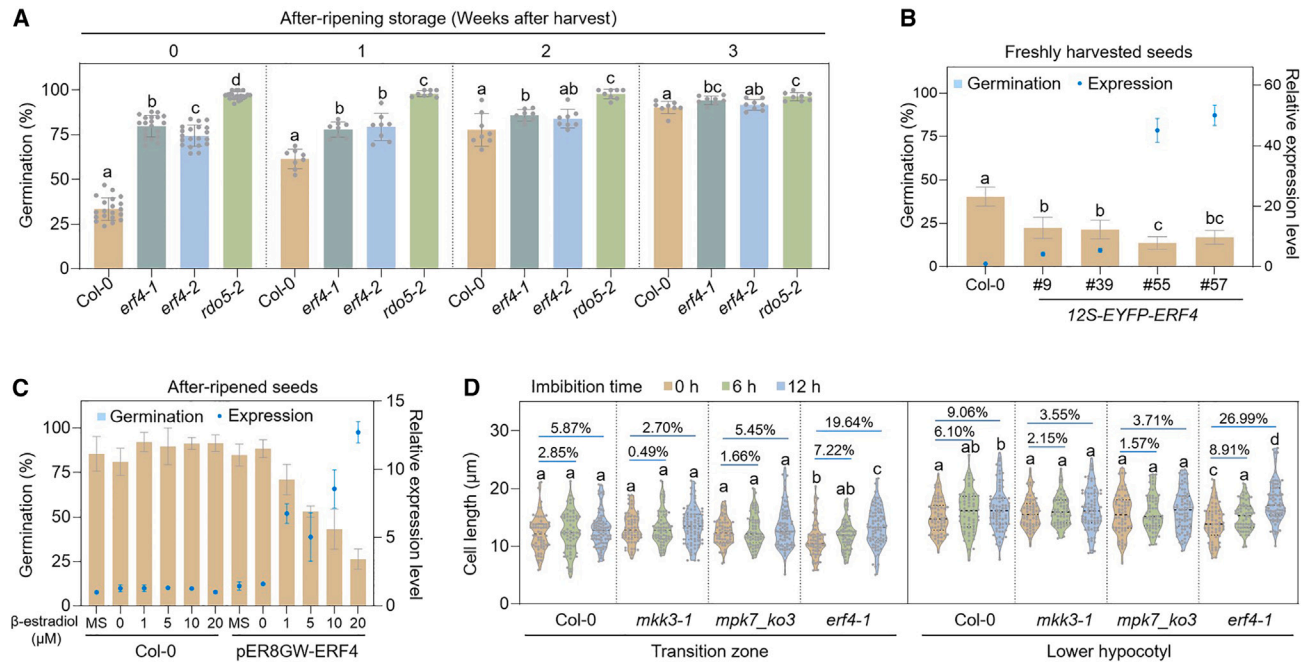


Figure 5. ERF4 is a dormancy regulator that suppresses embryo expansion.

(A and B) Germination assays with seeds from *erf4-1* and *erf4-2* **(A)** or ERF4 overexpression lines **(B)**. The *rdo5-2* mutant was used as a non-dormant control in **(A)**. The germination rates were calculated after 7 days of incubation under 16-h light/8-h dark (23°C/20°C) conditions. Data are represented as means ± SD of at least six independent replicates. Each dot in **(A)** represents the value from one replicate. Lowercase letters indicate statistically distinct groups ($p < 0.05$, Student's *t*-test). The right y axis in **(B)** indicates the expression level of ERF4 in overexpression lines.

(C) Induced expression of ERF4 during imbibition reduces seed germination. After-ripened seeds were sown onto $\frac{1}{2}$ MS plates containing the indicated concentrations of β -estradiol. “0” refers to the plate containing the solvent in which β -estradiol was dissolved, which was used as a mock control. The germination rates were calculated after 7 days of incubation under 16-h light/8-h dark (23°C/20°C) conditions. Data are represented as means ± SD of three independent replicates. The right y axis shows the expression level of ERF4 after β -estradiol induction.

(D) Cell length and average cell elongation rate of the radicle-adjacent transition zone and lower hypocotyl of Col-0, *mkk3-1*, *mpk7_ko3*, and *erf4-1*. The length of at least 60 cells from each genotype was measured after 0-, 6-, and 12-h imbibition. Each dot represents the value from one cell. Numbers represent the average cell elongation rates, which were calculated by dividing the relative values of cell elongation after 6- or 12-h imbibition by the cell length at 0 h. See also [supplemental Figures 4 and 5](#).

et al., 2005; Ding et al., 2021, 2022). Through genome sequence analysis, we identified GCC box motifs in the exon regions of *EXPA1*, *EXPA8*, *EXPA9*, *EXPA13*, and *EXPA15*, and we performed a chromatin immunoprecipitation (ChIP)-qPCR assay to verify ERF4 binding to these motifs *in vivo*. The results showed that ERF4 associates with the GCC box motifs of these *EXPAs* (Figure 6B and 6C). These binding sites were consistent with an *in vitro* binding assay from the Plant Cistrome database ([supplemental Figure 6](#)) (O'Malley et al., 2016). We also performed an electrophoretic mobility shift assay (EMSA) to verify their direct binding and confirmed that recombinant His-ERF4 protein bound directly to these sequences (Figure 6B and 6D). Collectively, our results demonstrate that ERF4 can bind directly to GCC boxes in the exons of these *EXPA* genes and inhibit their expression.

Phosphorylation of ERF4 by MPK7 promotes ERF4 degradation to releases its inhibitory effect on *EXPA* expression and seed germination

During the Co-IP experiment, detection of YFP-ERF4 in 12S-EYFP-ERF4 transgenic seeds was challenging without pre-treatment with a buffer containing MG132, suggesting that ERF4 may be prone to degradation in seeds. We hypothesized

that phosphorylation of ERF4 by MPK7 might regulate its degradation, similar to that triggered by phosphorylation of ERF13 by MPK14 (Lv et al., 2021), a member of the same subfamily as MPK7. To investigate this possibility, we performed a series of cell-free degradation assays (Koyama et al., 2013). Initially, we incubated recombinant His-ERF4 protein with a seed protein extract solution with or without the proteasome inhibitor MG132 for 0–60 min to determine its degradation rate. In the absence of MG132, the abundance of His-ERF4 declined sharply after 15 min and disappeared completely after 30 min. However, addition of MG132 significantly delayed this degradation (Figure 7A), confirming that ERF4 degradation is rapid and dependent on the 26S proteasome. We next generated His-ERF4^{AAA} and His-ERF4^{DDD} fusion proteins to mimic non-phosphorylated and phosphorylated ERF4 by mutating the three putative serine (S) phosphorylation sites (S98, S109, and S173) to alanine (A) or aspartic acid (D), respectively. In similar cell-free degradation assays, the His-ERF4^{DDD} protein degraded the fastest, followed by His-ERF4^{WT}, but a significant residual amount of His-ERF4^{AAA} protein was still present within the tested time window (Figure 7B), indicating that phosphorylation promotes ERF4 degradation. Finally, we investigated whether loss of *MKK3* or *MPK7* function affects the degradation rate of ERF4 by incubating the same amount

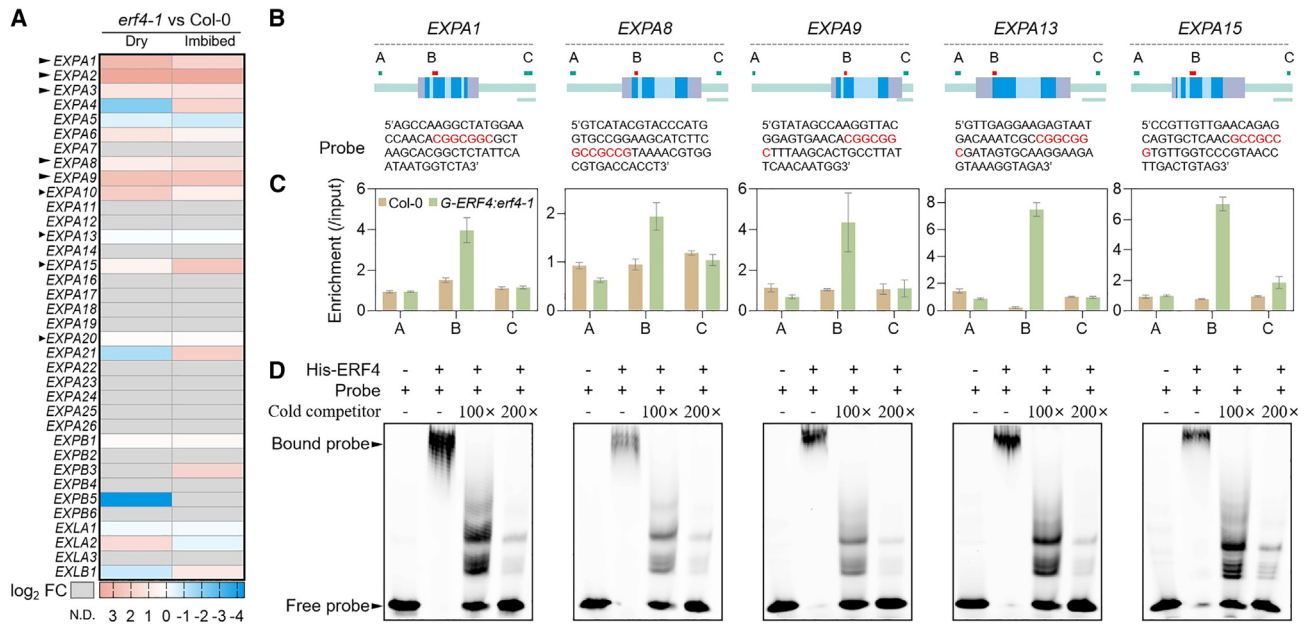


Figure 6. ERF4 directly binds to EXPAs and suppresses their expression.

(A) Heatmap showing changes in expression of EXP family members in dry and 6-h imbibed *erf4-1* seeds compared with Col-0 seeds. The heatmap is based on \log_2 (fold change) values from RNA-seq.

(B) Diagrams showing the locations of the regions detected in **(C)** and the probe sequences used in **(D)**. The gene structure is graphed to scale. Blue box, exon; cyan box, intron; lavender box, 5'/3' UTR. The detected regions are indicated by A, B, and C, and region B contains the GCC box. Bar, 500 bp.

(C) Detection of GFP-ERF4 binding sites on EXPAs by ChIP-qPCR assays. DNA samples were extracted from 7-day-old seedlings that constitutively expressed GFP-ERF4 driven by the 35S promoter. Col-0 was used as a negative control, and *ACTIN2* was used as an internal reference. The expression value of region A in Col-0 of replicate one was normalized as "1." Data are represented as means \pm SD of three independent replicates.

(D) EMSA assays confirm the binding of ERF4 to the EXPA genes *in vitro*. Probes were labeled with 6-carboxy-fluorescein (FAM). The corresponding probes without labels (cold competitors) were used as a control. Representative images of three replicates with similar results are shown. See also supplemental Figure 6.

of His-ERF4 protein with protein solutions extracted from Col-0, *mkk3-1*, and *mpk7_ko3* seeds. The results showed that both *mkk3-1* and *mpk7_ko3* mutant extracts significantly delayed the degradation of ERF4 (Figure 7C). Together, these results suggest that phosphorylation of ERF4 by the MKK3-MPK7 module regulates its degradation.

To solidify the genetic linkage, we generated the homozygous double mutant *mpk7_ko3 erf4-1* to verify whether ERF4 acts downstream of MPK7 in regulating seed dormancy. We compared the dormancy levels of Col-0, *mpk7_ko3*, *erf4-1*, and *mpk7_ko3 erf4-1* and found that loss of *ERF4* function significantly attenuated the enhanced dormancy level of *mpk7_ko3* (Figure 7D). Moreover, we compared the expression levels of EXPAs in imbibed seeds from different genetic backgrounds and found that, similar to its effects on seed dormancy, loss of *ERF4* function restored the reduced EXPA expression in *mpk7_ko3* (Figure 7E). It is important to emphasize that lack of *ERF4* function did not completely restore seed dormancy levels and expression of most EXPAs in the *mpk7_ko3* background to match those of the wild type. This observation strongly suggests that additional downstream regulatory factors are influenced by MPK7. Collectively, these results suggest that phosphorylation of ERF4 by MPK7 promotes ERF4 degradation and thus releases its inhibitory effect on EXPA expression and seed germination.

DISCUSSION

Seeds have only one chance to germinate, and they have evolved complex ways to determine the optimal time for germination. Seed dormancy can prevent seed germination, enabling plants to avoid subsequent unsuitable conditions. During seed storage, seeds sense the surrounding environment and transduce these signals to adjust their dormancy state in order to commence their new life under optimal conditions. Therefore, seed plants should have evolved fate switches to determine their fate (Bassel, 2016).

Here, we make the case that the MKK3-MPK7 cascade, along with its downstream target ERF4, constitutes a fate switch that governs the transition from seed dormancy to germination. In our proposed model (Figure 7F), seeds produce certain signal molecules when they encounter suitable conditions for seed germination, and these activate the MKK3-MPK7 module (Figure 2A-2E), which subsequently phosphorylates ERF4 (Figure 4), leading to its rapid degradation (Figure 7A-7C). This, in turn, relieves the suppressive effect of ERF4 on the expression of several EXPAs (*EXPA1*, *EXPA8*, *EXPA9*, and *EXPA15*) (Figures 3 and 6) that are critical for promoting cell expansion during seed imbibition (Cosgrove, 1998; 2000; Schopfer, 2001; Holdsworth et al., 2008; Zhong et al., 2015; Xu et al., 2020). The MKK3-MPK7-ERF4-EXPA axis is mainly

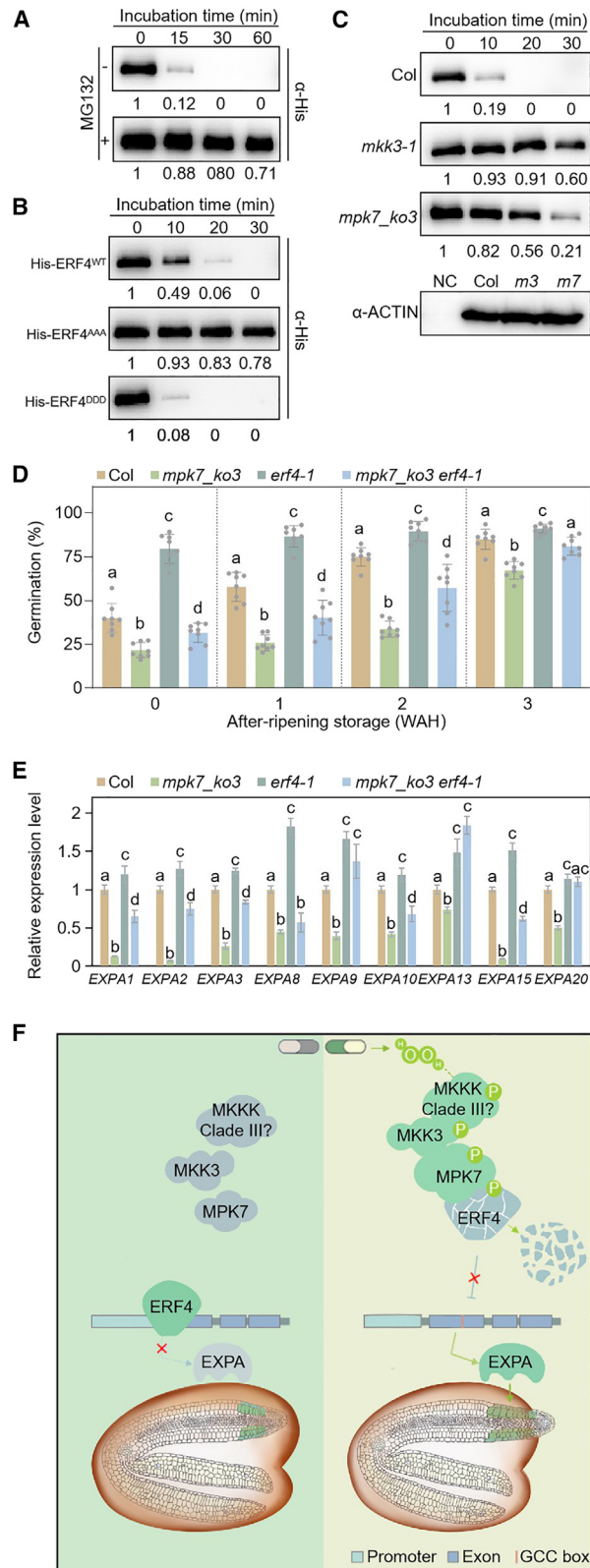


Figure 7. Phosphorylation of ERF4 by MPK7 promotes ERF4 degradation to releases its inhibitory effect on EXPA expression and seed germination.

(A–C) Cell-free degradation assays detect the degradation kinetics of His-ERF4.

involved in the process of dormancy breaking and is distinct from the pathway(s) controlled by ABA and DOG1/RDO5 (Figure 2F–2H; supplemental Figure 2), which are mainly involved in the process of dormancy establishment (Bentsink et al., 2006; Nakabayashi et al., 2012; Xiang et al., 2014; Née et al., 2017a; Soppe and Bentsink, 2020).

We propose that H₂O₂ may be one of the upstream signaling molecules that activate the MKK3-centered cascade. Seeds produce a significant amount of H₂O₂ during imbibition and after-ripening, as well as after GA and CS treatments (Oracz et al., 2009; Leymarie et al., 2012; Bailly, 2019; Jurdak et al., 2022). H₂O₂ can activate the MKK3-MPK7 module (Figure 2E; Doczi et al., 2007), and the MKK3-MPK7 module is required for the response to these dormancy-breaking conditions or treatments (Figure 2A–2C). In addition, *in vivo* assays have demonstrated that H₂O₂ can also activate MPK1 and MPK2 (Ortiz-Masia et al., 2007), which are direct downstream MPKs of MKK3. However, it is still unclear how H₂O₂ can activate the MKK3-centered cascade. One possible approach to address this question is to investigate the relationship between H₂O₂ and MKK3 upstream of MKK3. Previous studies have shown that MKK3 interacts with six of the eight clade III MKKs in *Arabidopsis* (Danquah et al., 2015; Matsuoka et al., 2015; Colcombet et al., 2016). Therefore, future studies could focus on clade III MKKs to investigate the relationship between H₂O₂ and activity of these MKKs.

(A) His-ERF4 protein was incubated with seed protein extracted from Col-0, with or without 50 μ M MG132, for the indicated times.

(B) His-ERF4, His-ERF4^{AAA}, and His-ERF4^{DDD} were incubated with seed protein extracted from Col-0 for the indicated times.

(C) His-ERF4 protein was incubated with seed protein extracted from Col-0, *mkk3-1*, and *mpk7_ko3* for the indicated times. The abundance of His-MPK7 was detected with an anti-His antibody. Numbers indicate the relative gray value of the His-MPK7 band calculated with ImageJ. The value of the sample “0 min” was normalized as “1.” A representative image of three replicates with similar results is shown. The internal control confirmed that the protein extract solutions from Col-0, *mkk3-1* (*m3*), and *mpk7_ko3* (*m7*) had the same protein quantities. Protein extraction buffer was used as a negative control (NC).

(D) Germination assays with seeds from different genetic backgrounds. The germination rates were calculated after 7 days of incubation under 16-h light/8-h dark (23°C/20°C) conditions. Data are represented as means \pm SD of at least six independent replicates. Each dot represents the value from one replicate. Lowercase letters indicate statistically distinct groups ($p < 0.05$, Student’s *t*-test).

(E) Expression of *EXPAs* in imbibed seeds of Col-0, *mpk7_ko3*, *erf4-1*, and *mpk7_ko3 erf4-1* detected by qRT-PCR. *ACTIN8* was used as an internal reference. Data are represented as means \pm SD of three independent replicates. Lowercase letters indicate statistically distinct groups ($p < 0.05$, Student’s *t*-test).

(F) A working model of the MKK3-MPK7-ERF4-EXPA axis in dormancy breaking. Under conditions unsuitable for seed germination (left panel), ERF4 binds to the GCC boxes in the exons of some *EXPAs* and inhibits their transcription. The seeds maintain their dormant state. Under conditions suitable for seed germination (right panel), cells generate the signal molecule H₂O₂, which activates the MKK3-MPK7 module. The activated module phosphorylates ERF4, leads to its degradation, and relieves its suppressive effect on expression of the *EXPAs*. The *EXPAs* then promote cell expansion in the radicle-adjacent transition zone and lower hypocotyl, which leads to radicle protrusion. Therefore, MKK3-MPK7-ERF4 works as a fate switch that is flipped on by signal molecules produced under conditions suitable for seed germination, thereby governing the transition from seed dormancy to germination.

MKK3-MPK7-ERF4 axis regulates seed dormancy

Molecular Plant

Our findings suggest that MPK7 is the predominant direct downstream MPK of MKK3 in seed dormancy regulation of *Arabidopsis* (Figure 1B–1D; supplemental Figure 1D). In rice, MPK14 is also considered to be a downstream MPK of MKK3 in regulation of seed dormancy (Mao et al., 2019). Given their high sequence similarity, we hypothesize that MPK14 may share some common substrates with MPK7 (Hamel et al., 2006) and may thus participate in dormancy regulation like MPK7, as seed-specific overexpression of MPK14 can reduce seed dormancy (Li et al., 2019). However, in *Arabidopsis*, the contribution of MPK14 to seed dormancy regulation is much lower than that of MPK7: *MPK14* expression in seeds is extremely low, and the *mpk14* mutant displays no dormancy-related phenotypes (Figure 1B–1D; supplemental Figure 1D). In addition, because the phenotype of *mpk7_ko3* was less pronounced than that of *mkk3-1* in terms of seed germination, gene expression, and cell elongation (Figures 2A–2C, 2G, and 3A–3C), other MPKs downstream of MKK3, including indirect ones, may also play a role in this dormancy-breaking pathway. For example, although MPK8 did not interact directly with MKK3 in yeast two-hybrid assays (Doczi et al., 2007; Lee et al., 2008), it can be activated by the MKK3-mediated cascade and promote seed germination (Takahashi et al., 2011; Zhang et al., 2019). Therefore, it is MKK3, rather than upstream MKKs or downstream MPKs, that is the center of this functional module. This is consistent with previous findings, which indicated that MKK3 is the causal gene for the major dormancy QTL of barley and wheat (Nakamura et al., 2016; Torada et al., 2016).

In our study, we identified the novel seed dormancy regulator ERF4, which regulates the release of dormancy during seed imbibition by acting downstream of MPK7 (Figures 4, 5, and 7). We found that ERF4 suppresses the expression of several EXPAs that facilitate embryo expansion during seed imbibition by binding to GCC box motifs in their exons (Figure 6; supplemental Figure 6). Our results provide further experimental support for previous reports suggesting that cis-acting elements in the exon region rather than the promoter region also regulate gene expression (de Vooght et al., 2008; Zhao et al., 2015; Ding et al., 2021). ERF4 has been reported to interact with TCP15 and inhibit its promotion of gene transcription (Ding et al., 2022). TCP15 and its homolog TCP14 have been shown to directly regulate the expression of *EXPA9* and to rely on *EXPA9* in GA-stimulated seed germination (Xu et al., 2020). Further investigation is required to determine whether ERF4 regulates *EXPA* expression through antagonism with TCP14 or TCP15. Moreover, TCP14 has been reported to be phosphorylated by MPK8 and to act as a module with MPK8 in promoting seed germination (Zhang et al., 2019). Therefore, MKK3-MPK7/MPK8, TCP14/TCP15, ERF4, and EXPAs may form an extraordinarily sophisticated network for regulation of dormancy breaking and seed germination. Further biochemical and genetic data are required to clarify their intricate relationship.

Our results highlight the importance of the kinase activity of the MKK3-MPK7 module for dormancy regulation. These findings are consistent with previous observations in wheat and barley, in which nonsynonymous amino acid substitutions in the kinase domain of MKK3 affected both kinase activity and seed dormancy level (Nakamura et al., 2016; Torada et al., 2016). Our experimental observation that MKK3-MPK7-mediated phos-

phorylation promotes the degradation of ERF4 is consistent with previous reports. For example, ERF4-GFP was shown to accumulate in nuclear bodies (Yang et al., 2005), which are proposed to be sites for protein degradation (Wang et al., 2001). Immunoblotting analysis using protein extracted from MG132-treated transgenic plants overexpressing ERF4-HA revealed an upper-shifted band corresponding to ERF4-HA (Koyama et al., 2013) that may correspond to the phosphorylated form of ERF4-HA. NtERF3, the tobacco homolog of ERF4, can be rapidly degraded within 15 min (Koyama et al., 2013), similarly to ERF4, whose turnover is about 20–30 min (Figure 7A–7C). Deletion of amino acid residues 83 to 190 of NtERF3 can slow its degradation through an unknown mechanism (Koyama et al., 2013). These residues may contain phosphorylation sites, as this sequence corresponds to the sequence where phosphorylation sites of ERF4 were identified in our study. Further studies are needed to gain a more comprehensive understanding of the mechanisms of protein degradation across different species, including the factors that regulate this process and the signaling pathways involved.

In conclusion, our work reveals the molecular mechanism by which the MKK3-MPK7-ERF4 module regulates the release of seed dormancy. This MKK3-centered dormancy-breaking pathway serves as a crucial mechanism by which seeds can sense and respond to germination-promoting signals, subsequently release dormancy, and initiate seed germination. Importantly, this pathway appears to be conserved among different species. It may therefore represent an important adaptive mechanism by which seed plants can ensure that their dormant offspring awaken and begin to grow and reproduce under suitable conditions.

METHODS

Plant materials and growth conditions

Arabidopsis thaliana materials used in this study were in the Col-0 or *Ler* background. The T-DNA insertion lines were ordered from the Nottingham Arabidopsis Stock Centre (<https://arabidopsis.info/BasicForm>) or AraShare (<https://www.arashare.cn>). The mapping of *ODR2* was completed in our previous work (Liu et al., 2020) and confirmed by Sanger sequencing. Details of all genetic materials and primer sequences used in this study are provided in supplemental Table 1.

Arabidopsis seeds were sown in a soil mixture and grown in a growth chamber (Hipoint, FH-1300) under a 16-h light/18-h dark cycle (23°C/20°C) with 55%–60% humidity. Freshly harvested seeds were immediately used for seed dormancy and germination assay or stored in a cabinet (Huayuxiandai, HYXD-180KWS) under constant conditions (dark, 50% humidity, 22°C) for after-ripening treatment.

Seed dormancy and germination assays

Seed dormancy levels were evaluated by measuring germination rates under suitable conditions during after-ripening storage (Soppe and Bentsink, 2020). The seeds were sown onto water-saturated filter papers, placed into a transparent moisturized container, and incubated in a germination cabinet (Hipoint, FH-650) for 7 days. The suitable germination conditions referred to in this study were a 16-h light/8-h dark (23°C/20°C) cycle with 55%–60% humidity. Radicle protrusion was used as the germination indicator. For GA treatment, filter papers were saturated with water containing different concentrations of GA. For CS treatment, containers were incubated in a 4°C refrigerator for different durations. For the H₂O₂ treatment,

Molecular Plant

seeds were pre-imbibed in water containing different concentrations of H₂O₂ for 6 h before being transferred to water-saturated filter papers. For ABA and β -estradiol treatments, seeds were sown on $\frac{1}{2}$ MS plates containing different concentrations of ABA or β -estradiol.

Plasmid construction and plant transformation

The full-length coding sequences (CDSs) of *ERF4*, *RDO5*, and *MPK7* were amplified and cloned into the pGEX4T1 or pET28a vector to express GST-tagged or His-tagged fusion proteins in *Escherichia coli*, respectively. The fusion PCR method was used for site-directed mutagenesis of *ERF4* and *MKK3*. The EGFP sequence was inserted into the pCAMBIA1305 vector to construct p1305-GFP. Subsequently, the CDSs of *ERF4*, *MKK3*, and the indicated *EXPA*s were amplified and cloned into the p1305-GFP vector to create constructs expressing GFP-tagged fusion proteins driven by the 35S promoter in *Arabidopsis* or *Nicotiana benthamiana*. CDSs of the prey and bait genes were inserted into the pGADT7 or pGBKT7 vector, respectively, for yeast two-hybrid assays.

The pCAMBIA1300-pYAO-Cas9-AtU6-26-sgRNA^{MPK7} plasmid was constructed following the instructions of the pYAO-based CRISPR–Cas9 system (Yan et al., 2015) to generate genome-edited knockout lines of *MPK7* in the Col-0 background. The 12S-EYFP-ERF4 plasmid was constructed following the instructions of the GreenGate system (Lamprouopoulos et al., 2013) to generate lines with seed-specific overexpression of the YFP-ERF4 fusion protein. The pFAST-R05-MKK3/MKK3^{EE}/MPK7 plasmid was constructed following the instructions of the FAST system (Shimada et al., 2010) to generate overexpression lines of *MKK3*, *MKK3*^{EE}, and *MPK7*. Sequences of all constructs were confirmed by Sanger sequencing. Supplemental Table 1 lists all primers used for construction.

All binary constructs were introduced into *Agrobacterium tumefaciens* strain GV3101 (WEIDI, AC1001) for *Arabidopsis* transformation by the floral dip method (Clough and Bent, 1998). T3 homozygous single-insertion lines were selected for further analysis.

qRT-PCR and RNA-seq analyses

Total RNA was extracted from freshly harvested dry or 6-h imbibed seeds using the FastPure Plant Total RNA Isolation Kit (Vazyme, RC401) according to the manufacturer's instructions. For qRT-PCR assays, the RNA sample was treated with DNase I to remove residual genomic DNA and served as the template for reverse transcription using the HiScript III 1st Strand cDNA Synthesis Kit (Vazyme, R312-01). Quantitative real-time PCR was performed using ChamQ Universal SYBR qPCR Master Mix (Vazyme, Q711). Relative gene expression was analyzed using the 2^{- $\Delta\Delta$ Ct} method with *ACTIN8* (AT1G49240) as an internal reference. For RNA-seq analysis, library preparation and paired-end, 150-bp sequencing were completed at Novogene Biotech (Beijing, China) using an Illumina NovaSeq 6000 instrument. The raw data were analyzed as described in our previous work (Li et al., 2022): first, low-quality sequences were removed using fastp (version 0.20.0, -z 4-q 20 -u 30 -n 10); second, clean reads were mapped to the *Arabidopsis* reference genome using HISAT2 (version 2.1.0); third, featureCounts (version 2.0.1) was used to count the reads with the parameters -p -t exon -g gene_id; fourth, the raw counts were normalized with DESeq2 (version 1.34.0) to compare gene expression between different samples. The transcripts per million value was used to represent RNA abundance of a particular gene in order to eliminate statistical biases among various samples (Li and Dewey, 2011; Wagner et al., 2012).

Protein expression, extraction, and purification

The BL21 (DE3) strain was used to express GST- or His-tagged fusion proteins in *E. coli*, and GFP-tagged fusion proteins were expressed in *N. benthamiana*. For protein expression in BL21, an overnight culture of BL21 harboring corresponding expression constructs was diluted in 200 ml LB medium. The culture was grown at 37°C to an OD₆₀₀ of 0.6–0.8, supplemented with 1 mM IPTG, and shaken for another 3 h. Cells were har-

MKK3–MPK7–ERF4 axis regulates seed dormancy

vested by centrifugation at 4000 g and 4°C for 15 min. For protein expression in tobacco, the GV3101 strain harboring the corresponding expression constructs was transfected into tobacco leaves as described previously (Sparkes et al., 2006). After 1–3 days of culture, fluorescent areas detected with a portable GFP excitation light source (LUYOR, 3415RG) were cut out and treated as indicated. The successfully expressed *E. coli* or tobacco samples were quickly frozen in liquid nitrogen and stored at –80°C until further extraction.

For proteins extracted from *E. coli*, the cell pellets were resuspended using lysis buffer (140 mM NaCl, 2.7 mM KCl, 10 mM Na₂HPO₄, 1.8 mM KH₂PO₄ [pH 7.3] for GST-tagged fusion proteins; 20 mM phosphate buffer, 500 mM NaCl, 10 mM imidazole [pH 7.4] for His-tagged proteins) and disrupted with a high-pressure cell disruptor (JNBIO, JN-02C). For proteins extracted from tobacco or *Arabidopsis*, samples were ground in liquid nitrogen and suspended in the indicated extraction buffer. All cell debris was removed by centrifugation at 12 000 g and 4°C for 20 min. The supernatant was collected for subsequent purification.

Proteins were purified using Ni²⁺ Magarose beads (Solarbio, M2300) for His-tagged proteins, GST resin (TransGen, DP201-01) for GST-tagged proteins, and anti-GFP nanobody Magarose beads (Ktsm, KTSM1334) for GFP-tagged proteins following the users' manuals. Protein concentrations were measured with a Bradford Protein Assay Kit (GBCBIO, G3155-1) and adjusted to 0.5–1 μ g/ μ l using Protein Concentrators (Thermo Scientific, 88513) with the indicated exchanging buffer.

Quantitative analyses of protein abundance

Protein samples were extracted from seeds with seed protein extraction buffer (100 mM Tris–Cl [pH 7.5], 6 M urea, 2 M thiourea, 0.05% [v/v] Triton X-100, 0.2% [w/v] sarcosyl, 2 mM DTT). Protein abundance was quantified by immunoblotting using the corresponding specific antibody. The anti-DOG1 and anti-RDO5 antibodies were raised in rabbits by YOUKE (Shanghai, China), and the anti-MPK7 antibody (Doczi et al., 2007) was purchased from PhytoAB (PHY0866A). As an internal reference, the abundance of plant actin was detected using an anti-plant actin antibody (Affinity, T0015). Protein abundance was quantified from the gray value of the band using ImageJ software (<https://imagej.net/ij/>).

Quantitative analyses of MPK7 protein activity

The total proteins were extracted from Col-0 seeds using protein extraction buffer (50 mM Tris–HCl [pH 7.5], 150 mM NaCl, 1% [v/v] Triton X-100, 50 μ M MgCl₂, 1 mM DTT, 1 mM ATP, protease inhibitor cocktail [Yeasen, 20124ES03], phosphatase inhibitor cocktail [Yeasen, 20109ES05]). The buffer in which His-MPK7 or total protein was dissolved was exchanged for a kinase buffer (50 mM Tris–HCl [pH 7.5], 10 mM MgCl₂, 1 mM DTT, 1 mM ATP) using Protein Concentrators (Thermo Scientific, 88513). The kinase reaction was performed by incubating the His-MPK7 protein (2 μ g) with total protein at 37°C for 30 min and terminated by adding an equal volume of 2 \times SDS loading buffer. Phosphorylated His-MPK7 was detected by immunoblotting using an anti-pTEpY antibody (Promega, V8031). The abundance of His-MPK7, detected with an anti-His antibody (Proteintech, 66005-1-Ig), was used as an internal reference. Protein abundance was quantified from the gray value of the band using ImageJ software. MPK7 activity was quantified by calculating the gray value ratio of pTEpY to His using ImageJ software.

Measurement of cell length

Seeds were imbibed on water-saturated filter papers under suitable conditions. Embryos were dissected from their seed coats with forceps using a microscope (Olympus, SZX7). Isolated embryos were stained in 10 μ M propidium iodide for 10 min and then rinsed in water. Samples were transferred to slides, and photos were taken using a confocal microscope (Leica, SP8). The radicle-adjacent transition zone and lower hypocotyl region were determined as described previously (Sliwinska et al., 2009). For measurement of cell length, four plants of each genotype were

MKK3-MPK7-ERF4 axis regulates seed dormancy

Molecular Plant

measured as biological replicates. For each plant, three to four embryos were measured to capture the variability within the genetic material. Within each embryo, the lengths of five individual cells were measured to obtain representative data.

Yeast two-hybrid assays

The CDSs of *DOG1*, *RDO5*, and *MPK7* were inserted into the pGBKT7 vector as bait, and those of *MKK3*, *RDO5*, *DOG1*, and *ERF4* were inserted into the pGADT7 vector as prey. The yeast strain Y187 (WEIDI, YC1020S) was used for yeast transformation, which was performed using a Frozen-EZ Yeast Transformation II Kit (Zymo Research, T2001) following the user's manual. For the yeast two-hybrid library screen, construction of the TF library in *Arabidopsis* and screening of the yeast two-hybrid library were completed by OE Biotech (Shanghai, China).

GFP pull-down assays

A bead mixture containing the GFP-ERF4 protein was incubated with the GST-MPK7 and GST-RDO5 protein at 4°C for 3 h. The pull-down reaction was stopped by resuspending the beads in 1× SDS loading buffer after washing them five times. The proteins were detected by immunoblotting with anti-GST (TransGen, HT601-01) and anti-GFP (TransGen, HT801-01) antibodies.

Co-IP assays

Seeds of the indicated genetic materials were imbibed in protein enrichment buffer (50 mM MES [pH 5.7], 0.05% [v/v] Tween 20, 50 μM MG132) for 12 h. Total proteins were extracted using protein extraction buffer (50 mM Tris-HCl [pH 7.5], 150 mM NaCl, 1% [v/v] Triton X-100, protease inhibitor cocktail [Yeasen, 20124ES03], 50 μM MG132). The Co-IP reaction was performed by incubating the total protein with anti-GFP nanobody Magarose beads (Ktsm, KTSM1334) for 3 h at 4°C and stopped by resuspending the beads in 1× SDS loading buffer after washing them five times. The proteins were detected by immunoblotting with anti-GFP (TransGen, HT801-01) and anti-MPK7 (PhytoAB, PHY0866A) antibodies.

Non-radioactive *in vitro* labeling assays

Recombinant His-MPK7, His-ERF4, and His-ERF4^{AAA} were purified from BL21. The GFP-MKK3 fusion protein was expressed in tobacco leaves and extracted after 0.3% H₂O₂ treatment for 30 min. The His-MPK7 protein was pre-activated by activated GFP-MKK3 before the non-radioactive labeling assay. In brief, His-MPK7 immobilized on beads were incubated with activated GFP-MKK3 in a kinase buffer (50 mM Tris-HCl [pH 7.5], 10 mM MgCl₂, 1 mM DTT, 1 mM ATP) at 37°C for 30 min. Residual GFP-MKK3 was removed by extensively washing the active His-MPK7-bound beads and confirmed with a portable GFP excitation light source (LUYOR, 3415RG). The eluted active His-MPK7 was then used to perform non-radioactive *in vitro* labeling assays as described previously, with minor modifications (Leissing et al., 2016). In brief, the thiophosphorylation reaction was performed by mixing 200 ng active His-MPK7 with 1 μg His-ERF4 or His-ERF4^{AAA} in a kinase reaction containing 1 mM ATP_γS (Abcam, ab138911) for 1 h and stopped by adding 20 mM EDTA. The alkylation reaction of the thiophosphorylated substrate was performed by adding 2.5 mM PNBM (Abcam, ab138910) in 5% (v/v) DMSO for 2 h and stopped by adding an equal volume of 2× SDS loading buffer. The thiophosphorylated proteins and the His-MPK7 protein were detected by anti-TPE (Abcam, ab92570) and anti-His (Proteintech, 66005-1-Ig) antibodies, respectively, and His-MPK7 was used as a loading control.

ChIP-qPCR assays

ChIP was performed as described previously, with minor modifications (Gendrel et al., 2005). Seven-day-old seedlings of 35S-GFP-ERF4:*erf4-1* with detectable GFP signal were sampled. Samples were cross-linked with 1% formaldehyde for 15 min under a vacuum, and the reaction was stopped with a final concentration of 0.125 M glycine for 5 min. After the sample was ground into a homogeneous powder, chromatin was isolated

and sheared to 300–1000 bp by sonication. Immunoprecipitation was performed with an anti-GFP antibody (Abcam, ab290) and protein A/G beads. The cross-linking was then reversed, and the immunoprecipitated DNA was recovered and analyzed by qPCR with specific primers (supplemental Table 1).

EMSAs

Recombinant His-ERF4 fusion protein was purified from BL21. The 6-carboxy-fluorescein (FAM)-labeled double-stranded DNAs (FAM probes) were generated by annealing two primers whose sequence information is listed in supplemental Table 1. Probes without labels were used as cold competitors. EMSAs were performed according to the instructions of the LightShift Chemiluminescent EMSA Kit (Thermo Fisher Scientific, 20148). Fluorescence images were obtained with a Multispectral laser imager (Amersham Typhoon, FLA 9500).

In vitro degradation assays

The cell-free degradation assay was performed as described previously, with some modifications (Koyama et al., 2013). A solution containing eluted proteins was exchanged for a buffer containing 20 mM Tris and 100 mM NaCl. To prepare the extract solution, 15 mg of seeds were ground in liquid nitrogen, suspended in degradation buffer (50 mM Tris-HCl [pH 7.5], 10 mM NaCl, 10 mM MgCl₂, 5 mM dithiothreitol, 2 mM ATP, protease inhibitor cocktail [Yeasen, 20124ES03], phosphatase inhibitor cocktail [Yeasen, 20109ES05]), and centrifuged at 12 000 g and 4°C for 30 min. The supernatant was the cell extract solution. The degradation assay was performed by incubating aliquots containing 1 μg recombinant protein and 800 μg cell extract protein with or without an additional 50 μM MG132 at 37°C for the indicated time periods. The reaction was terminated by adding an equal volume of 2× SDS loading buffer. The proteins were detected by immunoblotting with anti-His antibody (Proteintech, 66005-1-Ig).

DATA AVAILABILITY

The RNA-seq data reported in this study have been deposited in the Gene Expression Omnibus database (www.ncbi.nlm.nih.gov/geo/) under accession numbers GSE230257 and GSE230392. Sequence data from this article can be found at TAIR (<https://www.arabidopsis.org/>) under the following accession numbers: *MKK3* (AT5G40440), *MPK1* (AT1G10210), *MPK2* (AT1G59580), *MPK7* (AT2G18170), *MPK14* (AT4G36450), *ERF4* (AT3G15210), *EXPA1* (AT1G69530), *EXPA2* (AT5G05290), *EXPA3* (AT2G37640), *EXPA8* (AT2G40610), *EXPA9* (AT5G02260), *EXPA10* (AT1G26770), *EXPA13* (AT3G03220), *EXPA15* (AT2G03090), *EXPA20* (AT4G38210), *DOG1* (AT5G45830), *RDO5* (AT4G11040), *ACTIN8* (AT1G49240), and *ACTIN2* (AT3G18780).

SUPPLEMENTAL INFORMATION

Supplemental information is available at *Molecular Plant Online*.

FUNDING

This work was supported by the National Natural Science Foundation of China (grant nos. 32000250 and 32170364), the China Postdoctoral Science Foundation (grant no. 2020M682997), the Key Area Research and Development Program of Guangdong Province (grant no. 2021B0707010006), the Science, Technology and Innovation Commission of Shenzhen Municipality (grant nos. KCXFZ-20201221173203009 and KCXFZ-20211020164207012), and the Dapeng New District Science and Technology Program (grant nos. KJYF202101-09 and RCTD20180102).

AUTHOR CONTRIBUTIONS

Conceptualization, X.C., Q.L., and Y.X.; methodology, X.C. and Q.L.; validation, X.C., Q.L., and S.Z.; investigation, X.C., Q.L., S.Z., S.S., L.D., X.X., W.J., B.Z., L.Z., Y. Lian, X.K., X.D., J.Z., and C.L.; resources, L.D.,

Molecular Plant

W.J.J.S., and Y.X.; data curation, X.C., Q.L., and Y.X.; writing – original draft, X.C. and Q.L.; writing – review & editing, X.C., Q.L., W.J.J.S., and Y.X.; visualization, Y. Luo; supervision, Y.X.; project administration, X.C., Q.L., and Y.X.; funding acquisition, X.C. and Y.X.

ACKNOWLEDGMENTS

We thank Dr. Kazumi Nakabayashi for the YFP-DOG1 seeds. We thank Dr. Yingzhen Kong and Dr. Anming Ding for ERF4-related genetic materials. The authors declare no competing interests.

Received: April 15, 2023

Revised: August 18, 2023

Accepted: September 11, 2023

REFERENCES

- Arc, E., Chibani, K., Grappin, P., Jullien, M., Godin, B., Cueff, G., Valot, B., Balliau, T., Job, D., and Rajjou, L. (2012). Cold stratification and exogenous nitrates entail similar functional proteome adjustments during *Arabidopsis* seed dormancy release. *J. Proteome Res.* **11**:5418–5432.
- Asai, T., Tena, G., Plotnikova, J., Willmann, M.R., Chiu, W.L., Gomez-Gomez, L., Boller, T., Ausubel, F.M., and Sheen, J. (2002). MAP kinase signalling cascade in *Arabidopsis* innate immunity. *Nature* **415**:977–983.
- Bai, F., and Matton, D.P. (2018). The *Arabidopsis* Mitogen-Activated Protein Kinase Kinase Kinase 20 (MKKK20) C-terminal domain interacts with MKK3 and harbors a typical DEF mammalian MAP kinase docking site. *Plant Signal. Behav.* **13**, e1503498.
- Bailey, C. (2019). The signalling role of ROS in the regulation of seed germination and dormancy. *Biochem. J.* **476**:3019–3032.
- Baskin, J.M., and Baskin, C.C. (2004). A classification system for seed dormancy. *Seed Sci. Res.* **14**:1–16.
- Bassel, G.W. (2016). To Grow or not to Grow? *Trends Plant Sci.* **21**:498–505.
- Bassel, G.W., Stamm, P., Mosca, G., Barbier de Reuille, P., Gibbs, D.J., Winter, R., Janka, A., Holdsworth, M.J., and Smith, R.S. (2014). Mechanical constraints imposed by 3D cellular geometry and arrangement modulate growth patterns in the *Arabidopsis* embryo. *Proc. Natl. Acad. Sci. USA* **111**:8685–8690.
- Benhamman, R., Bai, F., Drory, S.B., Loubert-Hudon, A., Ellis, B., and Matton, D.P. (2017). The *Arabidopsis* Mitogen-Activated Protein Kinase Kinase Kinase 20 (MKKK20) Acts Upstream of MKK3 and MPK18 in Two Separate Signaling Pathways Involved in Root Microtubule Functions. *Front. Plant Sci.* **8**:1352.
- Bentsink, L., Jowett, J., Hanhart, C.J., and Koornneef, M. (2006). Cloning of *DOG1*, a quantitative trait locus controlling seed dormancy in *Arabidopsis*. *Proc. Natl. Acad. Sci. USA* **103**:17042–17047.
- Bewley, J.D. (1997). Seed Germination and Dormancy. *Plant Cell* **9**:1055–1066.
- Bryant, F.M., Hughes, D., Hassani-Pak, K., and Eastmond, P.J. (2019). Basic LEUCINE ZIPPER TRANSCRIPTION FACTOR67 Transactivates *DELAY OF GERMINATION1* to Establish Primary Seed Dormancy in *Arabidopsis*. *Plant Cell* **31**:1276–1288.
- Cao, F.Y., DeFalco, T.A., Moeder, W., Li, B., Gong, Y., Liu, X.M., Taniguchi, M., Lumba, S., Toh, S., Shan, L., et al. (2018). *Arabidopsis* ETHYLENE RESPONSE FACTOR 8 (ERF8) has dual functions in ABA signaling and immunity. *BMC Plant Biol.* **18**:211.
- Chen, N., Wang, H., Abdelmageed, H., Veerappan, V., Tadege, M., and Allen, R.D. (2020). HSI2/VAL1 and HSL1/VAL2 function redundantly to repress *DOG1* expression in *Arabidopsis* seeds and seedlings. *New Phytol.* **227**:840–856.
- Choi, S.W., Lee, S.B., Na, Y.J., Jeung, S.G., and Kim, S.Y. (2017). *Arabidopsis* MAP3K16 and Other Salt-Inducible MAP3Ks Regulate ABA Response Redundantly. *Mol. Cell* **40**:230–242.
- Clough, S.J., and Bent, A.F. (1998). Floral dip: a simplified method for *Agrobacterium*-mediated transformation of *Arabidopsis thaliana*. *Plant J.* **16**:735–743.
- Coego, A., Brizuela, E., Castillejo, P., Ruíz, S., Koncz, C., del Pozo, J.C., Piñeiro, M., Jarillo, J.A., Paz-Ares, J., and León, J.; TRANSPLANTA Consortium (2014). The TRANSPLANTA collection of *Arabidopsis* lines: a resource for functional analysis of transcription factors based on their conditional overexpression. *Plant J.* **77**:944–953.
- Colcombet, J., and Hirt, H. (2008). *Arabidopsis* MAPKs: a complex signalling network involved in multiple biological processes. *Biochem. J.* **413**:217–226.
- Colcombet, J., Sözen, C., and Hirt, H. (2016). Convergence of Multiple MAP3Ks on MKK3 Identifies a Set of Novel Stress MAPK Modules. *Front. Plant Sci.* **7**:1941.
- Cosgrove, D.J. (1998). Cell wall loosening by expansins. *Plant Physiol.* **118**:333–339.
- Cosgrove, D.J. (2000). Loosening of plant cell walls by expansins. *Nature* **407**:321–326.
- Danquah, A., de Zélicourt, A., Boudsocq, M., Neubauer, J., Frei Dit Frey, N., Leonhardt, N., Pateyron, S., Gwinner, F., Tamby, J.P., Ortiz-Masia, D., et al. (2015). Identification and characterization of an ABA-activated MAP kinase cascade in *Arabidopsis thaliana*. *Plant J.* **82**:232–244.
- de Vooght, K.M.K., van Wijk, R., and van Solinge, W.W. (2008). GATA-1 binding sites in exon 1 direct erythroid-specific transcription of PPOX. *Gene* **409**:83–91.
- Debeaujon, I., Léon-Kloosterziel, K.M., and Koornneef, M. (2000). Influence of the testa on seed dormancy, germination, and longevity in *Arabidopsis*. *Plant Physiol.* **122**:403–414.
- Dębska, K., Krasuska, U., Budnicka, K., Bogatek, R., and Gniazdowska, A. (2013). Dormancy removal of apple seeds by cold stratification is associated with fluctuation in H₂O₂, NO production and protein carbonylation level. *J. Plant Physiol.* **170**:480–488.
- Ding, A., Tang, X., Yang, D., Wang, M., Ren, A., Xu, Z., Hu, R., Zhou, G., O'Neill, M., and Kong, Y. (2021). ERF4 and MYB52 transcription factors play antagonistic roles in regulating homogalacturonan demethylesterification in *Arabidopsis* seed coat mucilage. *Plant Cell* **33**:381–403.
- Ding, A.M., Xu, C.T., Xie, Q., Zhang, M.J., Yan, N., Dai, C.B., Lv, J., Cui, M.M., Wang, W.F., and Sun, Y.H. (2022). ERF4 interacts with and antagonizes TCP15 in regulating endoreduplication and cell growth in *Arabidopsis*. *J. Integr. Plant Biol.* **64**:1673–1689.
- Dóczy, R., Brader, G., Pettkó-Szandtner, A., Rajh, I., Djamei, A., Pitzschke, A., Teige, M., and Hirt, H. (2007). The *Arabidopsis* mitogen-activated protein kinase kinase MKK3 is upstream of group C mitogen-activated protein kinases and participates in pathogen signaling. *Plant Cell* **19**:3266–3279.
- Fujimoto, S.Y., Ohta, M., Usui, A., Shinshi, H., and Ohme-Takagi, M. (2000). *Arabidopsis* ethylene-responsive element binding factors act as transcriptional activators or repressors of GCC box-mediated gene expression. *Plant Cell* **12**:393–404.
- Gendrel, A.V., Lippman, Z., Martienssen, R., and Colot, V. (2005). Profiling histone modification patterns in plants using genomic tiling microarrays. *Nat. Methods* **2**:213–218.

MKK3-MPK7-ERF4 axis regulates seed dormancy

Molecular Plant

- Hamel, L.P., Nicole, M.C., Sritubtim, S., Morency, M.J., Ellis, M., Ehling, J., Beaudoin, N., Barbazuk, B., Klæssig, D., Lee, J., et al. (2006). Ancient signals: comparative genomics of plant MAPK and MAPKK gene families. *Trends Plant Sci.* **11**:192–198.
- Holdsworth, M.J., Bentsink, L., and Soppe, W.J.J. (2008). Molecular networks regulating *Arabidopsis* seed maturation, after-ripening, dormancy and germination. *New Phytol.* **179**:33–54.
- Hwa, C.M., and Yang, X.C. (2008). The AtMKK3 pathway mediates ABA and salt signaling in *Arabidopsis*. *Acta Physiol. Plant.* **30**:277–286.
- Jalmi, S.K., and Sinha, A.K. (2016). Functional Involvement of a Mitogen Activated Protein Kinase Module, OsMKK3-OsMPK7-OsWRK30 in Mediating Resistance against *Xanthomonas oryzae* in Rice. *Sci. Rep.* **6**, 37974.
- Jurdak, R., Rodrigues, G.d.A.G., Chaumont, N., Schivre, G., Bourbousse, C., Barneche, F., Bou Dagher Kharrat, M., and Bailly, C. (2022). Intracellular reactive oxygen species trafficking participates in seed dormancy alleviation in *Arabidopsis* seeds. *New Phytol.* **234**:850–866.
- Koornneef, M., Bentsink, L., and Hilhorst, H. (2002). Seed dormancy and germination. *Curr. Opin. Plant Biol.* **5**:33–36.
- Koyama, T., Nii, H., Mitsuda, N., Ohta, M., Kitajima, S., Ohme-Takagi, M., and Sato, F. (2013). A regulatory cascade involving class II ETHYLENE RESPONSE FACTOR transcriptional repressors operates in the progression of leaf senescence. *Plant Physiol.* **162**:991–1005.
- Lampropoulos, A., Sutikovic, Z., Wenzl, C., Maegele, I., Lohmann, J.U., and Forner, J. (2013). GreenGate - a novel, versatile, and efficient cloning system for plant transgenesis. *PLoS One* **8**, e83043.
- Lee, J.S., Huh, K.W., Bhargava, A., and Ellis, B.E. (2008). Comprehensive analysis of protein-protein interactions between *Arabidopsis* MAPKs and MAPK kinases helps define potential MAPK signalling modules. *Plant Signal. Behav.* **3**:1037–1041.
- Leissing, F., Nomoto, M., Bocola, M., Schwaneberg, U., Tada, Y., Conrath, U., and Beckers, G.J.M. (2016). Substrate thiophosphorylation by *Arabidopsis* mitogen-activated protein kinases. *BMC Plant Biol.* **16**:48.
- Leymarie, J., Vitkauskaitė, G., Hoang, H.H., Gendreau, E., Chazole, V., Meimoun, P., Corbineau, F., El-Maarouf-Bouteau, H., and Bailly, C. (2012). Role of reactive oxygen species in the regulation of *Arabidopsis* seed dormancy. *Plant Cell Physiol.* **53**:96–106.
- Li, B., and Dewey, C.N. (2011). RSEM: accurate transcript quantification from RNA-Seq data with or without a reference genome. *BMC Bioinf.* **12**:323.
- Li, Q., Chen, X., Zhang, S., Shan, S., and Xiang, Y. (2022). DELAY OF GERMINATION 1, the Master Regulator of Seed Dormancy, Integrates the Regulatory Network of Phytohormones at the Transcriptional Level to Control Seed Dormancy. *Curr. Issues Mol. Biol.* **44**:6205–6217.
- Li, X., Chen, T., Li, Y., Wang, Z., Cao, H., Chen, F., Li, Y., Soppe, W.J.J., Li, W., and Liu, Y. (2019). ETR1/RDO3 Regulates Seed Dormancy by Relieving the Inhibitory Effect of the ERF12-TPL Complex on *DELAY OF GERMINATION1* Expression. *Plant Cell* **31**:832–847.
- Liu, F., Zhang, H., Ding, L., Soppe, W.J.J., and Xiang, Y. (2020). REVERSAL OF RDO5 1, a Homolog of Rice Seed Dormancy4, Interacts with bHLH57 and Controls ABA Biosynthesis and Seed Dormancy in *Arabidopsis*. *Plant Cell* **32**:1933–1948.
- Liu, Y., Ye, N., Liu, R., Chen, M., and Zhang, J. (2010). H₂O₂ mediates the regulation of ABA catabolism and GA biosynthesis in *Arabidopsis* seed dormancy and germination. *J. Exp. Bot.* **61**:2979–2990.
- Lv, B., Wei, K., Hu, K., Tian, T., Zhang, F., Yu, Z., Zhang, D., Su, Y., Sang, Y., Zhang, X., and Ding, Z. (2021). MPK14-mediated auxin signaling controls lateral root development via ERF13-regulated very-long-chain fatty acid biosynthesis. *Mol. Plant* **14**:285–297.
- Mao, X., Zhang, J., Liu, W., Yan, S., Liu, Q., Fu, H., Zhao, J., Huang, W., Dong, J., Zhang, S., et al. (2019). The MKKK62-MKK3-MAPK7/14 module negatively regulates seed dormancy in rice. *Rice* **12**:2.
- Matsuoka, D., Yasufuku, T., Furuya, T., and Nanmori, T. (2015). An abscisic acid inducible *Arabidopsis* MAPKKK, MAPKKK18 regulates leaf senescence via its kinase activity. *Plant Mol. Biol.* **87**:565–575.
- Mortensen, S.A., and Grasser, K.D. (2014). The seed dormancy defect of *Arabidopsis* mutants lacking the transcript elongation factor TFIIS is caused by reduced expression of the *DOG1* gene. *FEBS Lett.* **588**:47–51.
- Müller, K., Linkies, A., Vreeburg, R.A.M., Fry, S.C., Krieger-Liszskay, A., and Leubner-Metzger, G. (2009). *In vivo* cell wall loosening by hydroxyl radicals during cross seed germination and elongation growth. *Plant Physiol.* **150**:1855–1865.
- Nakabayashi, K., Bartsch, M., Xiang, Y., Miatton, E., Pellengahr, S., Yano, R., Seo, M., and Soppe, W.J.J. (2012). The time required for dormancy release in *Arabidopsis* is determined by DELAY OF GERMINATION1 protein levels in freshly harvested seeds. *Plant Cell* **24**:2826–2838.
- Nakamura, S., Pourkheirandish, M., Morishige, H., Kubo, Y., Nakamura, M., Ichimura, K., Seo, S., Kanamori, H., Wu, J., Ando, T., et al. (2016). Mitogen-Activated Protein Kinase Kinase 3 Regulates Seed Dormancy in Barley. *Curr. Biol.* **26**:775–781.
- Nakano, T., Suzuki, K., Fujimura, T., and Shinshi, H. (2006). Genome-wide analysis of the *ERF* gene family in *Arabidopsis* and rice. *Plant Physiol.* **140**:411–432.
- Née, G., Xiang, Y., and Soppe, W.J. (2017a). The release of dormancy, a wake-up call for seeds to germinate. *Curr. Opin. Plant Biol.* **35**:8–14.
- Née, G., Kramer, K., Nakabayashi, K., Yuan, B., Xiang, Y., Miatton, E., Finkemeier, I., and Soppe, W.J.J. (2017b). DELAY OF GERMINATION1 requires PP2C phosphatases of the ABA signalling pathway to control seed dormancy. *Nat. Commun.* **8**:72.
- Nishimura, N., Yoshida, T., Kitahata, N., Asami, T., Shinozaki, K., and Hirayama, T. (2007). *ABA-Hypersensitive Germination1* encodes a protein phosphatase 2C, an essential component of abscisic acid signaling in *Arabidopsis* seed. *Plant J.* **50**:935–949.
- Ohta, M., Matsui, K., Hiratsu, K., Shinshi, H., and Ohme-Takagi, M. (2001). Repression domains of class II ERF transcriptional repressors share an essential motif for active repression. *Plant Cell* **13**:1959–1968.
- O'Malley, R.C., Huang, S.S.C., Song, L., Lewsey, M.G., Bartlett, A., Nery, J.R., Galli, M., Gallavotti, A., and Ecker, J.R. (2016). Cistrome and Epicistrome Features Shape the Regulatory DNA Landscape. *Cell* **165**:1280–1292.
- Oracz, K., El-Maarouf-Bouteau, H., Kranner, I., Bogatek, R., Corbineau, F., and Bailly, C. (2009). The mechanisms involved in seed dormancy alleviation by hydrogen cyanide unravel the role of reactive oxygen species as key factors of cellular signaling during germination. *Plant Physiol.* **150**:494–505.
- Ortiz-Masia, D., Perez-Amador, M.A., Carbonell, J., and Marcote, M.J. (2007). Diverse stress signals activate the C1 subgroup MAP kinases of *Arabidopsis*. *FEBS Lett.* **581**:1834–1840.
- Popescu, S.C., Popescu, G.V., Bachan, S., Zhang, Z., Gerstein, M., Snyder, M., and Dinesh-Kumar, S.P. (2009). MAPK target networks in *Arabidopsis thaliana* revealed using functional protein microarrays. *Genes Dev.* **23**:80–92.
- Rodriguez, M.C.S., Petersen, M., and Mundy, J. (2010). Mitogen-activated protein kinase signaling in plants. *Annu. Rev. Plant Biol.* **61**:621–649.
- Schopfer, P. (2001). Hydroxyl radical-induced cell-wall loosening *in vitro* and *in vivo*: implications for the control of elongation growth. *Plant J.* **28**:679–688.

Molecular Plant

- Sethi, V., Raghuram, B., Sinha, A.K., and Chattopadhyay, S.** (2014). A mitogen-activated protein kinase cascade module, MKK3-MPK6 and MYC2, is involved in blue light-mediated seedling development in *Arabidopsis*. *Plant Cell* **26**:3343–3357.
- Sharrocks, A.D., Yang, S.H., and Galanis, A.** (2000). Docking domains and substrate-specificity determination for MAP kinases. *Trends Biochem. Sci.* **25**:448–453.
- Shimada, T.L., Shimada, T., and Hara-Nishimura, I.** (2010). A rapid and non-destructive screenable marker, FAST, for identifying transformed seeds of *Arabidopsis thaliana*. *Plant J.* **61**:519–528.
- Sliwinska, E., Bassel, G.W., and Bewley, J.D.** (2009). Germination of *Arabidopsis thaliana* seeds is not completed as a result of elongation of the radicle but of the adjacent transition zone and lower hypocotyl. *J. Exp. Bot.* **60**:3587–3594.
- Soppe, W.J.J., and Bentsink, L.** (2020). Seed dormancy back on track; its definition and regulation by DOG1. *New Phytol.* **228**:816–819.
- Sözen, C., Schenk, S.T., Boudsocq, M., Chardin, C., Almeida-Trapp, M., Krapp, A., Hirt, H., Mithöfer, A., and Colcombet, J.** (2020). Wounding and Insect Feeding Trigger Two Independent MAPK Pathways with Distinct Regulation and Kinetics. *Plant Cell* **32**:1988–2003.
- Sparkes, I.A., Runions, J., Kearns, A., and Hawes, C.** (2006). Rapid, transient expression of fluorescent fusion proteins in tobacco plants and generation of stably transformed plants. *Nat. Protoc.* **1**:2019–2025.
- Takahashi, F., Mizoguchi, T., Yoshida, R., Ichimura, K., and Shinozaki, K.** (2011). Calmodulin-dependent activation of MAP kinase for ROS homeostasis in *Arabidopsis*. *Mol. Cell* **41**:649–660.
- Takahashi, F., Yoshida, R., Ichimura, K., Mizoguchi, T., Seo, S., Yonezawa, M., Maruyama, K., Yamaguchi-Shinozaki, K., and Shinozaki, K.** (2007). The mitogen-activated protein kinase cascade MKK3-MPK6 is an important part of the jasmonate signal transduction pathway in *Arabidopsis*. *Plant Cell* **19**:805–818.
- Tena, G., Asai, T., Chiu, W.L., and Sheen, J.** (2001). Plant mitogen-activated protein kinase signaling cascades. *Curr. Opin. Plant Biol.* **4**:392–400.
- Torada, A., Koike, M., Ogawa, T., Takenouchi, Y., Tadamura, K., Wu, J., Matsumoto, T., Kawaura, K., and Ogihara, Y.** (2016). A Causal Gene for Seed Dormancy on Wheat Chromosome 4A Encodes a MAP Kinase Kinase. *Curr. Biol.* **26**:782–787.
- Wagner, G.P., Kin, K., and Lynch, V.J.** (2012). Measurement of mRNA abundance using RNA-seq data: RPKM measure is inconsistent among samples. *Theor. Biosci.* **131**:281–285.
- Wang, H., Ma, L.G., Li, J.M., Zhao, H.Y., and Deng, X.W.** (2001). Direct interaction of *Arabidopsis* cryptochromes with COP1 in light control development. *Science* **294**:154–158.
- MKK3-MPK7-ERF4 axis regulates seed dormancy**
- Wang, Z., Chen, F., Li, X., Cao, H., Ding, M., Zhang, C., Zuo, J., Xu, C., Xu, J., Deng, X., et al.** (2016). *Arabidopsis* seed germination speed is controlled by SNL histone deacetylase-binding factor-mediated regulation of AUX1. *Nat. Commun.* **7**, 13412.
- Xiang, Y., Nakabayashi, K., Ding, J., He, F., Bentsink, L., and Soppe, W.J.J.** (2014). *Reduced Dormancy5* encodes a protein phosphatase 2C that is required for seed dormancy in *Arabidopsis*. *Plant Cell* **26**:4362–4375.
- Xiang, Y., Song, B., Née, G., Kramer, K., Finkemeier, I., and Soppe, W.J.J.** (2016). Sequence Polymorphisms at the REDUCED DORMANCY5 Pseudophosphatase Underlie Natural Variation in *Arabidopsis* Dormancy. *Plant Physiol.* **171**:2659–2670.
- Xu, H., Lantzouni, O., Bruggink, T., Benjamins, R., Lanfermeijer, F., Denby, K., Schwechheimer, C., and Bassel, G.W.** (2020). A Molecular Signal Integration Network Underpinning *Arabidopsis* Seed Germination. *Curr. Biol.* **30**:3703–3712.e4.
- Xu, J., and Zhang, S.** (2015). Mitogen-activated protein kinase cascades in signaling plant growth and development. *Trends Plant Sci.* **20**:56–64.
- Yamauchi, Y., Ogawa, M., Kuwahara, A., Hanada, A., Kamiya, Y., and Yamaguchi, S.** (2004). Activation of gibberellin biosynthesis and response pathways by low temperature during imbibition of *Arabidopsis thaliana* seeds. *Plant Cell* **16**:367–378.
- Yan, L., Wei, S., Wu, Y., Hu, R., Li, H., Yang, W., and Xie, Q.** (2015). High-efficiency genome editing in *Arabidopsis* using YAO promoter-driven CRISPR/Cas9 system. *Mol. Plant* **8**:1820–1823.
- Yang, Z., Tian, L., Latoszek-Green, M., Brown, D., and Wu, K.** (2005). *Arabidopsis* ERF4 is a transcriptional repressor capable of modulating ethylene and abscisic acid responses. *Plant Mol. Biol.* **58**:585–596.
- Zhang, K., Zhang, Y., Ji, Y., Walck, J.L., and Tao, J.** (2020). Seed Biology of *Lepidium apetalum* (Brassicaceae), with Particular Reference to Dormancy and Mucilage Development. *Plants-Basel* **9**:333.
- Zhang, M., and Zhang, S.** (2022). Mitogen-activated protein kinase cascades in plant signaling. *J. Integr. Plant Biol.* **64**:301–341.
- Zhang, W., Cochet, F., Ponnaiah, M., Lebreton, S., Matheron, L., Pionneau, C., Boudsocq, M., Resentini, F., Huguet, S., Blázquez, M.Á., et al.** (2019). The MPK8-TCP14 pathway promotes seed germination in *Arabidopsis*. *Plant J.* **100**:677–692.
- Zhao, Y., Cheng, S., Song, Y., Huang, Y., Zhou, S., Liu, X., and Zhou, D.X.** (2015). The Interaction between Rice ERF3 and WOX11 Promotes Crown Root Development by Regulating Gene Expression Involved in Cytokinin Signaling. *Plant Cell* **27**:2469–2483.
- Zhong, C., Xu, H., Ye, S., Wang, S., Li, L., Zhang, S., and Wang, X.** (2015). *Gibberellic Acid-Stimulated Arabidopsis6* Serves as an Integrator of Gibberellin, Abscisic Acid, and Glucose Signaling during Seed Germination in *Arabidopsis*. *Plant Physiol.* **169**:2288–2303.